

Article

Receptor-Specific Delivery of Peptide Nucleic Acids Conjugated to Three Sequentially Linked N-Acetyl Galactosamine Moieties into Hepatocytes

Krishna N. Ganesh, Pramod Bhingardeve, Bharath Raj Madhanagopal,
prashant jain, Hemanth Naick, and Muthiah Manoharan

J. Org. Chem., **Just Accepted Manuscript** • DOI: 10.1021/acs.joc.0c00601 • Publication Date (Web): 12 Jun 2020

Downloaded from pubs.acs.org on June 13, 2020

Just Accepted

“Just Accepted” manuscripts have been peer-reviewed and accepted for publication. They are posted online prior to technical editing, formatting for publication and author proofing. The American Chemical Society provides “Just Accepted” as a service to the research community to expedite the dissemination of scientific material as soon as possible after acceptance. “Just Accepted” manuscripts appear in full in PDF format accompanied by an HTML abstract. “Just Accepted” manuscripts have been fully peer reviewed, but should not be considered the official version of record. They are citable by the Digital Object Identifier (DOI®). “Just Accepted” is an optional service offered to authors. Therefore, the “Just Accepted” Web site may not include all articles that will be published in the journal. After a manuscript is technically edited and formatted, it will be removed from the “Just Accepted” Web site and published as an ASAP article. Note that technical editing may introduce minor changes to the manuscript text and/or graphics which could affect content, and all legal disclaimers and ethical guidelines that apply to the journal pertain. ACS cannot be held responsible for errors or consequences arising from the use of information contained in these “Just Accepted” manuscripts.

Receptor-Specific Delivery of Peptide Nucleic Acids Conjugated to Three Sequentially Linked *N*-Acetyl Galactosamine Moieties into Hepatocytes

Pramod Bhingardev,¹ Bharath Raj Madhanagopal,² Hemanth Naick,² Prashant Jain,¹ Muthiah Manoharan³ and Krishna Ganesh^{1,2,*}

1. Indian Institute of Science Education and Research (IISER) Pune, Dr Homi Bhabha Road, Pune 411008, Maharashtra, India
2. Indian Institute of Science Education and Research (IISER) Tirupati, Karkambadi Road, Tirupati 517507, Andhra Pradesh, India
3. Alnylam Pharmaceuticals, Cambridge, Massachusetts 02142 USA.

*To whom correspondence should be addressed. kn.ganesh@iisertirupati.ac.in

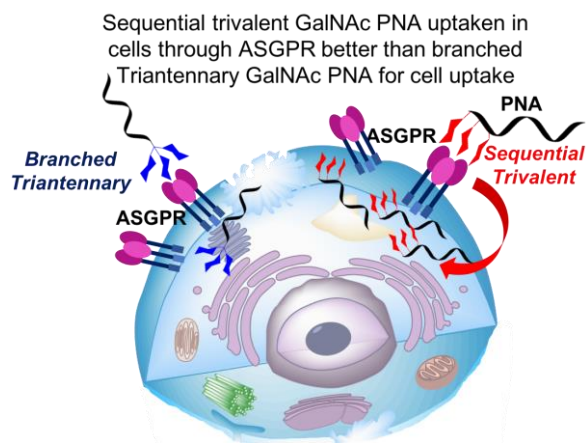
¹ PB. pramod.bhingardev@iiserpune.ac.in; PJ. prashant.jain@students.iiserpune.ac.in

² BM. madhang@iisertirupati.ac.in, HN. b.hemanth@iisertirupati.ac.in

³ MM. mmanoharan@alnylam.com

Table of contents

PNAs conjugated with *N*-acetyl galactosamine (GalNAc) in sequential vs. branched architecture



Keywords: *N*-acetyl galactosamine, GalNAc conjugate, peptide nucleic acid, hepatocyte, cellular uptake

Abstract

Peptide nucleic acids (PNAs) are DNA analogs that bind with high affinity to DNA and RNA in a sequence-specific manner but have poor cell permeability limiting use as therapeutic agents. The work described here is motivated by recent reports of efficient gene silencing specifically in hepatocytes by small interfering RNAs (siRNAs) conjugated to triantennary *N*-acetylgalactosamine (GalNAc), the ligand recognized by the asialoglycoprotein receptor (ASGPR). PNAs conjugated to either triantennary GalNAc at the N-terminus (the branched architecture) or to monomeric GalNAc moieties anchored at C γ of three consecutive PNA monomers of *N*-(2-aminoethyl)glycine (*aeg*) scaffolds (the sequential architecture) were synthesised on solid phase. These formed duplexes with complementary DNA and RNA as shown by UV and circular dichroism (CD) spectroscopy. The fluorescently labeled analogs of GalNAc-conjugated PNAs were internalized by HepG2 cells that express the ASGPR but were not taken up by HEK293 cells that lack this receptor. The sequential conjugate was internalized about 13-fold more efficiently than the branched conjugate into HepG2 cells as demonstrated by confocal microscopy. The results present here highlight the potential significance of the architecture of GalNAc conjugation for efficient uptake by target liver cells and indicate that GalNAc-conjugated PNAs have possible therapeutic applications.

Introduction

Antisense oligonucleotide therapeutics originate from the specific molecular recognition between the mRNA of the gene to be inhibited and synthetic single-stranded oligonucleotide drugs.¹⁻³ RNA interference (RNAi) is an endogenous pathway for post-transcriptional silencing of gene expression triggered by double-stranded RNAs including endogenous microRNAs and synthetic short interfering RNAs (siRNAs).⁴ As antisense oligonucleotide and siRNAs are too large and hydrophilic to diffuse across cell membranes on their own, uptake into target cells must be mediated by chemical modifications to the nucleic acid-based drug or adjuvants.⁵ The conjugation of triantennary N-acetyl galactosamine (GalNAc₃), which is the ligand for the asialoglycoprotein receptor (ASGPR), to siRNA duplexes or single-stranded antisense oligonucleotides enhances the potency of inhibition of gene expression in hepatocytes by 10 to 60 fold.^{6,7} Upon subcutaneous administration, a GalNAc₃-siRNA conjugate (Figure 1) robustly suppresses gene expression of the targeted mRNA in the liver of mice.⁶ It was also noted that conjugation of optimized chemically modified siRNAs to GalNAc₃ resulted in improved systemic stability against nucleases and favorable pharmacokinetics relative to the unconjugated siRNAs. The improved potency is a result of targeted delivery of the GalNAc₃-conjugated siRNA into hepatocytes via the ASGPR.⁸ This receptor is abundantly expressed almost exclusively on hepatocytes and clears glycoproteins and desialylated platelets from circulation.^{9,10} The first ever-approved oligonucleotide-GalNAc₃ conjugate is an RNAi therapeutic, Givosiran (GIVLAARI[®]), in which the sense strand of Givosiran siRNA is conjugated with GalNAc₃ for the treatment of acute hepatic porphyrias.¹¹ Numerous promising GalNAc-oligonucleotide conjugates are in clinical development.

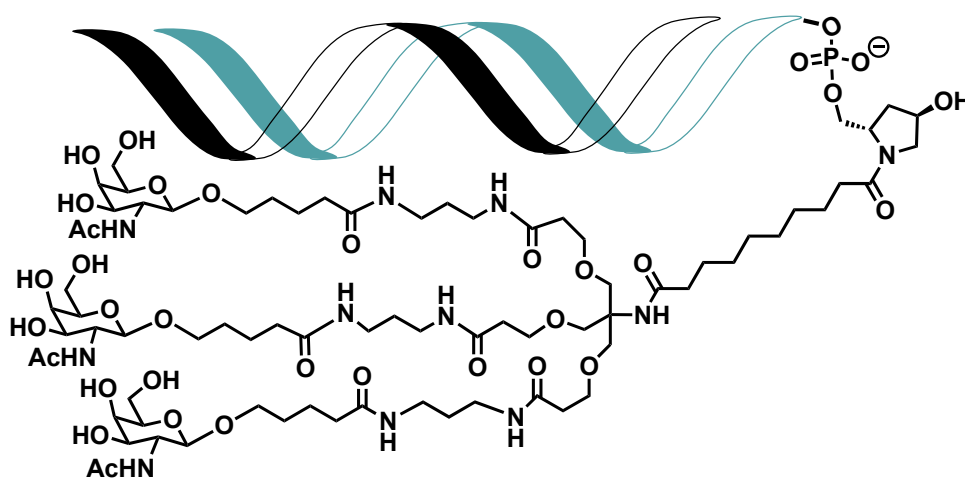


Figure 1. Structure of the GalNAc₃-siRNA conjugate

Peptide nucleic acids (ex. Figure 2, **PNA 1**) are DNA analogs that bind sequence specifically and with high affinity to both DNA and RNA.^{12,13} In PNAs, the nucleobases are linked via tertiary amide to an *N*2-aminoethylglycyl (*aeg*) backbone. Several PNA chemical modifications have been designed to improve their selectivity for DNA or RNA and to enhance their uptake into cells.¹⁴⁻¹⁹ Biessen *et al.* have reported the delivery of PNA conjugated to two GalNAc moieties into hepatocytes in a mouse model and have demonstrated reduction of expression of microsomal triglyceride transfer protein encoded by the targeted *MTP* mRNA.^{20,21} Motivated by the potency of GalNAc₃-conjugated siRNAs and antisense oligonucleotides in hepatocytes and subsequent approval of an RNAi therapeutic, we have synthesized two classes of PNA conjugates for evaluating their efficiency of their cell uptake. These are PNAs conjugated to triantennary GalNAc₃ through a spacer chain (“branched” conjugates, Figure 2, **PNA 2**) and a PNA in which GalNAc monomers are anchored to C^γ on the *aeg* backbone at three sequential PNA units at N-terminus, (“sequential” conjugates Figure 2, **PNA 3**) The sequential GalNAc PNA conjugates were designed to examine to what extent the linear substitution can mimic the geometry of branched GalNAc₃ in binding to the ASGPR on hepatocytes. In addition to synthesis of branched and sequential GalNAc-PNA conjugates and their fluorescent derivatives, this manuscript reports on efficiencies of their hybridization with DNA and RNA and relative uptake by cells that do and do not express the ASGPR. The sequential PNA analogue was more efficiently taken into cells than was the branched PNAs (Figure 2).

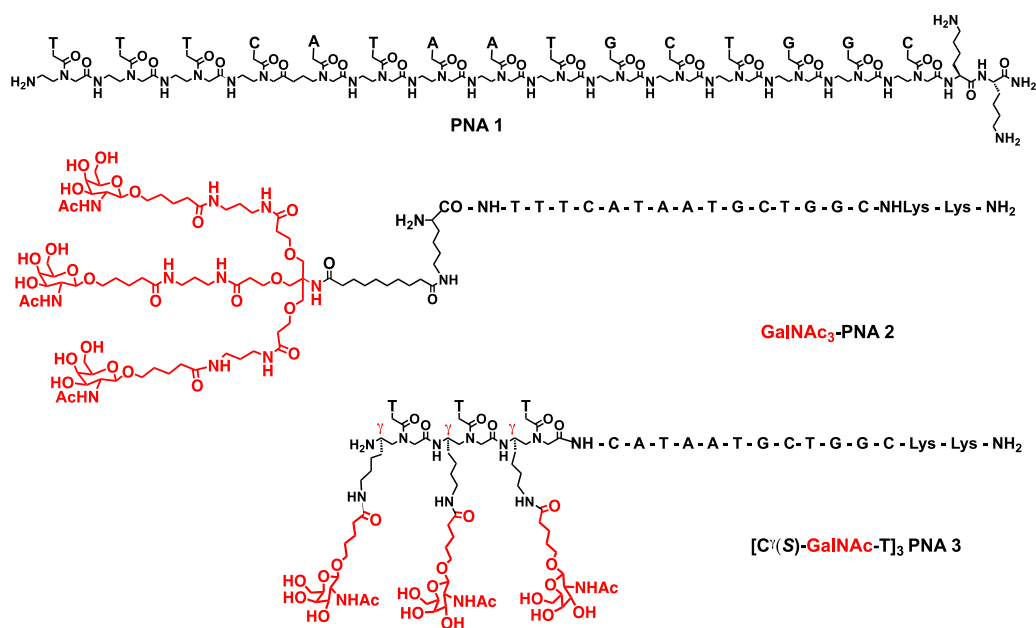


Figure 2. Structures of control, unconjugated **PNA 1**, branched GalNAc₃ conjugate **PNA 2**, and sequential GalNAc conjugate **PNA 3**

Results and Discussion

The synthesis of triantennary GalNAc₃ (**1c**) fragment (Figure 3) required for the synthesis of PNA **2** was done starting from the commercial D(+)-galactosamine to first obtain **1a** as per the literature procedure^{6,7,22} and then coupling with N,N'-protected lysine benzyl ester followed by debenzylation of ester to acid. The synthesis of [C^γ(S)-GalNAc-T]₃ PNA monomer (**2**) required for the synthesis of linear GalNAc conjugated PNA **3** was done starting from (ω-NHBoc)-(α-NHFmoc)-L-Lys-OH (**1**) (Scheme 1).

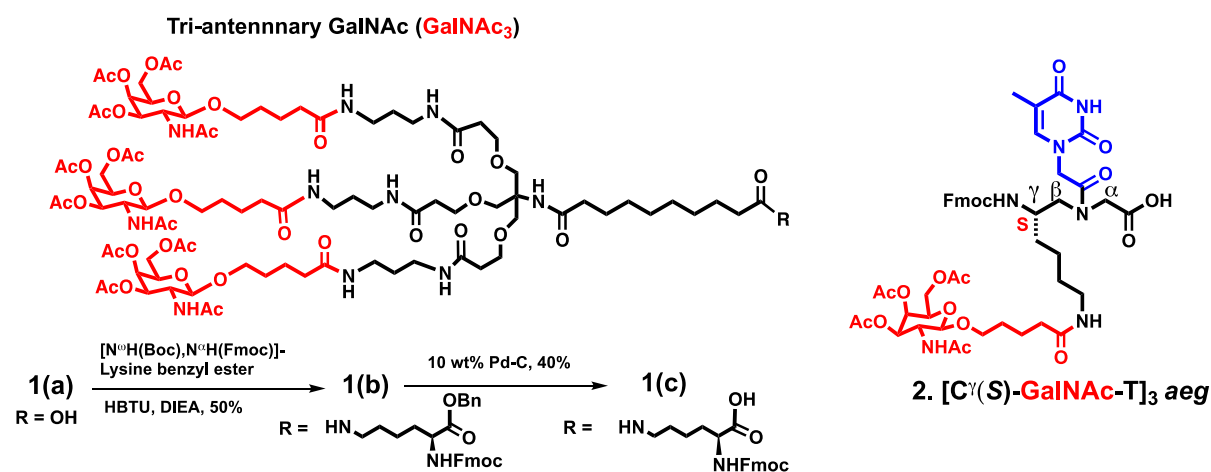


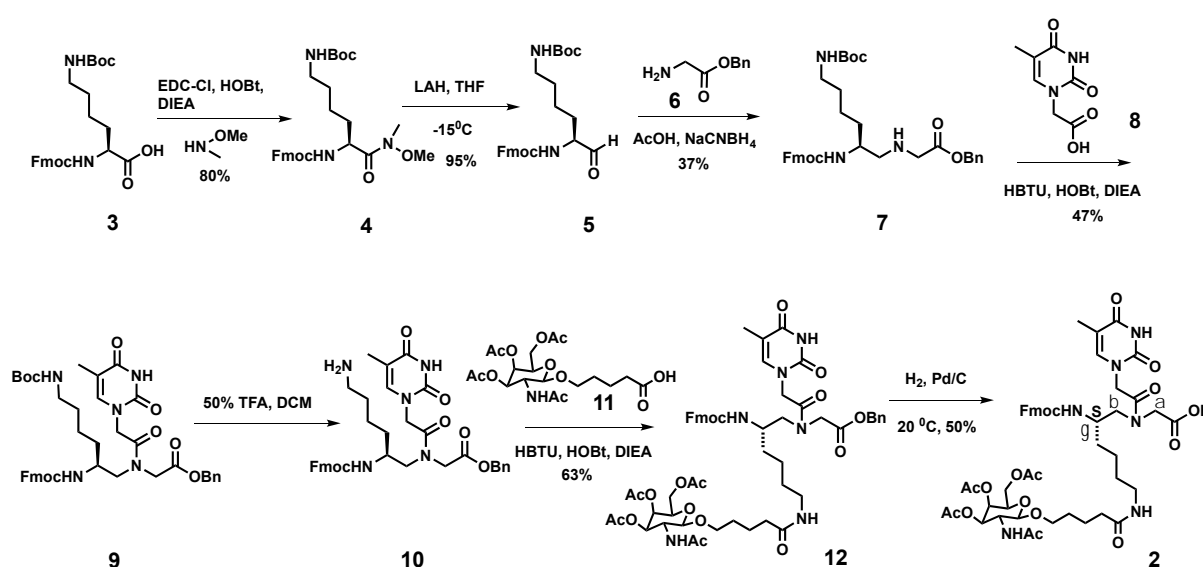
Figure 3. Chemical structures of target GalNAc monomers **1c** and **2** and synthesis of **1c**

The activation of acid function **3** by N,N-methoxymethyl amine gave the activated ester **4**, which was oxidized in the presence of lithium aluminum hydride in THF to obtain the aldehyde **5**. This was coupled with glycine benzyl ester under reductive amination conditions to obtain NHFmoc-[C^γ(S)-ω-NHBoc]-aminoethyl benzyl glycinate **7**. The coupling of thymine acetic acid **8** with amine **7** in the presence HBTU, HOBt and DIEA yielded C^γ(NHFmoc) (C^γS-butyl-4-NHBoc)-2-aminoethyl (N-acetamido-thyminy) glycy) benzyl ester **9**. The deprotection of NHBoc function gave the free amine **10**, which was coupled with 5-[3,4,6-tri-O-acetyl-2-(acetylamino)-2-deoxy-β-D-galactopyranosyl]oxy]-pentanoic acid⁷ (**11**) to yield the C^γ(S)-GalNAc substituted PNA-T ester **12**. Finally, catalytic hydrogenation of **12** over 10% Pd-C in the presence of acetic acid-methanol afforded the target C^γS-butyl-4-amido (GalNAc) aeg-PNA -T monomer **2**. All intermediate compounds were characterized by ¹H, ¹³C NMR and mass spectral data.

Synthesis of GalNAc-PNA oligomers. The synthesis of GalNAc conjugated PNA oligomers were done using standard solid phase synthesis protocol using Fmoc strategy (SI) on Rink amide resin. The assembly of PNA oligomer PNA **1** was done from C-terminus to the N-

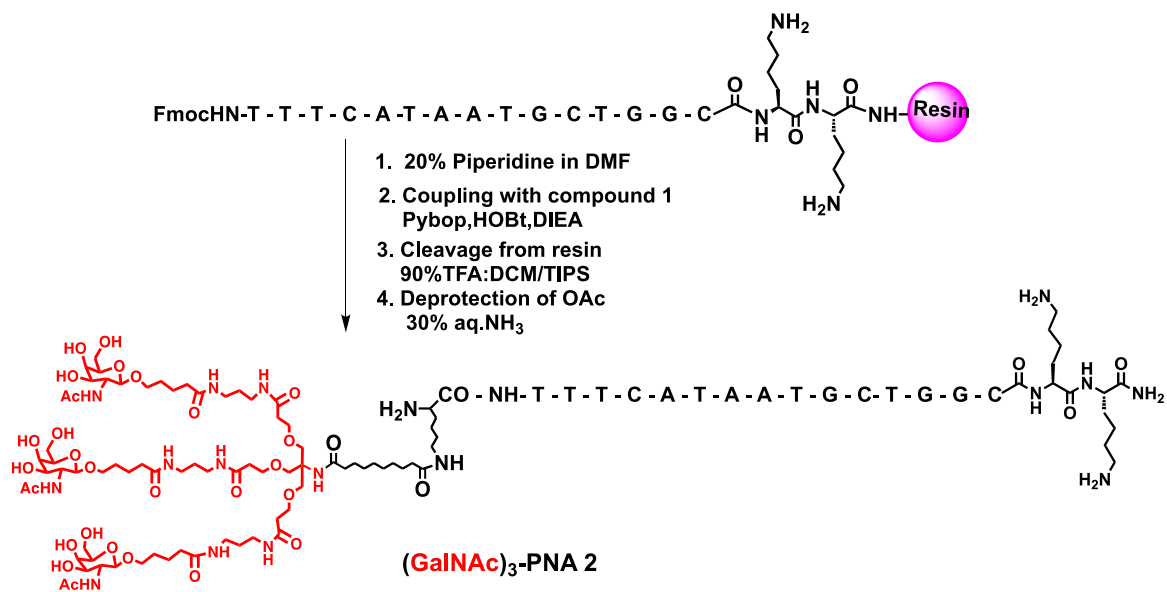
terminus using appropriate standard protected PNA (A/G/C/T) monomers.²³ The amino group on the resin was first coupled with orthogonally protected (C^α NHFmoc/ C^γ S-NH^oBoc)-L-lysine-OH²⁴⁻²⁷ at the C-terminus with *in situ* activation of acid with HBTU/HOBt, followed by removal of Fmoc by 20% piperidine in DMF treatment. The chain assembly was continued by sequential coupling with appropriate PNA monomers and deprotection using piperidine before each coupling step. At the end of **PNA 1** oligomer synthesis, additional coupling with the triantennary GalNAc₃ acid **1** using Pybop, HOBt and DIEA gave resin bound 15-mer GalNAc₃-PNA oligomer **PNA 2** (Scheme 2).

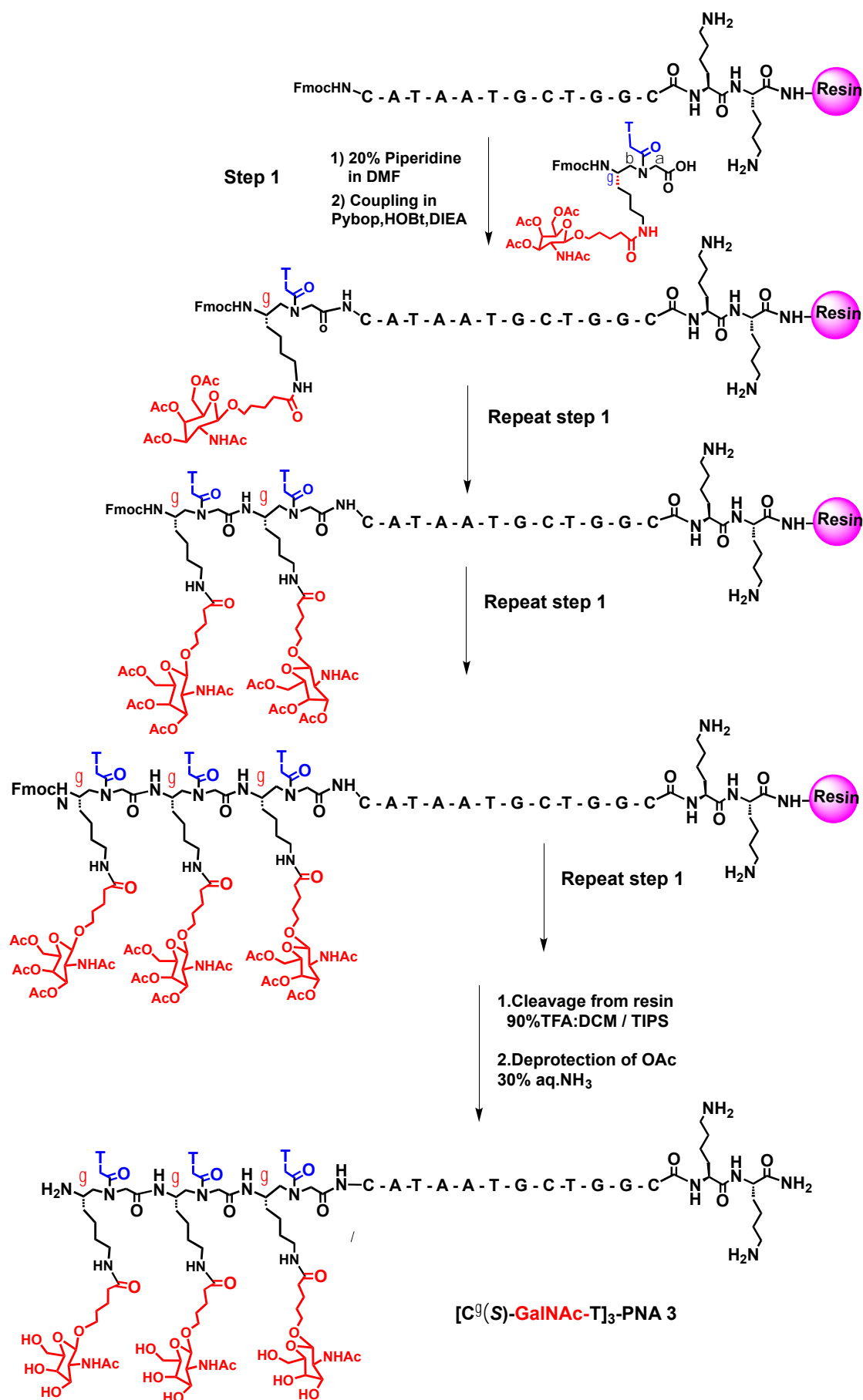
Scheme 1. Synthesis of C^γ (S)-butyl-4-amido(GalNAc).*aeg*.PNA-T monomer (**2**)



In a separate synthesis, after the completion of 12-mer PNA, three successive coupling cycles (coupling-deprotection) with GalNAc-PNA monomer **2** units, gave resin bound 15-mer [C^γ (S)-GalNAc-T]₃-PNA **3** in which one GalNAc fragment is attached to each of the 3 terminal PNA-T units at C^γ through a butylamido spacer chain (Scheme 3). The corresponding fluorescent PNA oligomers *Cf*-PNA **4**, *Cf*-GalNAc₃-PNA **5** and *Cf*-[C^γ (S)-GalNAc-T]₃-PNA **6**, required for cell permeation studies were synthesized after the final coupling of PNA oligomers at N-terminus with GalNAc derivative and deprotection of terminal NHFmoc on resin by DIEA and coupling with 5/6-carboxy fluorescein using Pybop and HOBt. The unmodified **PNA 1** without any N-terminal GalNAc unit, and its fluorescent derivative **PNA 4** were synthesized in a similar way as control PNAs for biochemical and biophysical studies.

Scheme 2. Solid phase synthesis of (GalNAc)₃-PNA **2**



Scheme 3. Solid phase synthesis of $[C^g(S)\text{-GalNAc-T}]_3\text{-PNA } \mathbf{3}$ 

After the assembly, all PNA oligomers were cleaved from the solid support (L-lysine derivatized Rink amide resin), using TFA in DCM in the presence of TIPS to yield completely deprotected PNA oligomers having L-lysine amides at their C-termini. The PNA oligomers in solution were precipitated by addition of cold diethyl ether and purified by semi-preparative C18 reverse phase high performance liquid chromatography (RP-HPLC). The purity of PNA oligomers was re-checked by analytical C18 RP column and characterized by MALDI-TOF mass spectral data (Table 1).

The fluorescent oligonucleotides *Cf*-PNA **4**, *Cf*-GalNAc₃-PNA **5** and *Cf*[C^γ(S)-GalNAc-T]₃-PNA **6** need for cell uptake studies were synthesised on solid support as shown in Scheme 4 and characterised by mass spectrometry data (Table 1). The UV absorption spectra of fluorescent PNAs showed absorbance maxima at 260 nm due to nucleobases and a lower intensity broad absorbance with maxima at 458 nm and 484 nm which are indicative of the presence of 5(6)-carboxyfluorescein in the PNA oligomers (Supporting Information, S33).

Scheme 4. Synthesis of fluorescent PNA oligomers

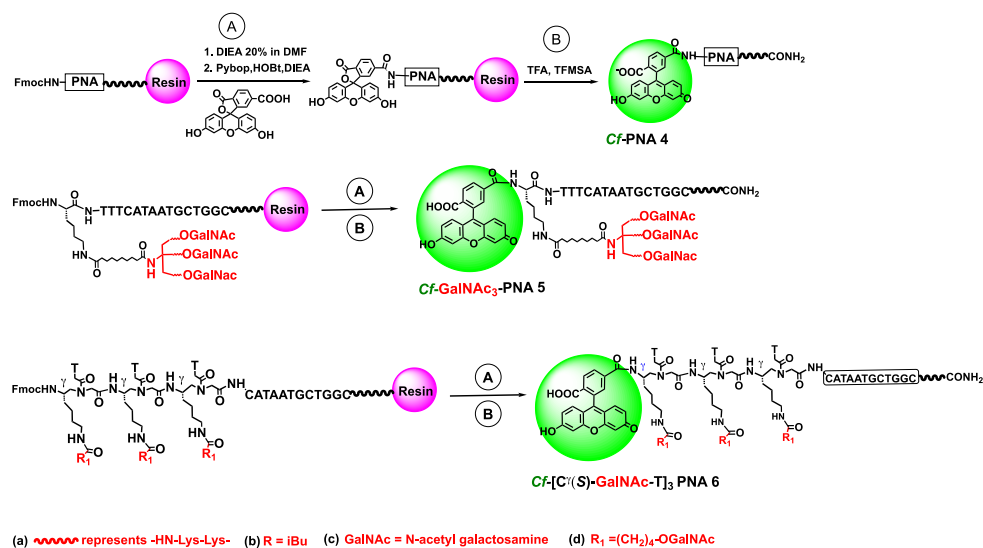


Table 1. MALDI-TOF spectral analysis of the synthesized PNA oligomers

Sr. No.	PNA sequence Code	Molecular Formula	Calc Mass	Obs Mass	Rt (min)
1	PNA 1	C ₁₇₄ H ₂₂₈ N ₈₆ O ₅₀	4321.77	4321.26	14.2
2	GalNAc ₃ -PNA 2	C ₂₄₅ H ₃₅₁ N ₉₅ O ₈₀	5907.08	5907.44	10.9
3	[C ^γ (S)-GalNAc-T] ₃ PNA 3	C ₂₂₅ H ₃₁₇ N ₉₁ O ₇₂	5448.57	5487.18[M + K] ⁺	11.5
4	<i>Cf</i> -PNA 4	C ₁₉₅ H ₂₃₈ N ₈₆ O ₅₆	4680.80	4681.60[M + H] ⁺	14.9
5	<i>Cf</i> -GalNAc ₃ -PNA 5	C ₂₇₂ H ₃₇₄ N ₉₈ O ₈₆	6392.58	6392.86	11.2

6	$C[C^{\gamma}(S)\text{-GalNAc-T}]_3$ PNA 6	$C_{246}H_{327}N_{91}O_{78}$	5806.88	5806.19	12.4
---	---	------------------------------	---------	---------	------

Incorporation of three GalNAc moieties in PNA was intended to aid the selective uptake of PNAs into hepatocytes that exhibit ASGPR on their surface. Since the utility of GalNAc₃ modified PNAs depends on whether or not they form stable PNA:RNA or PNA:DNA hybrids under physiological conditions, the thermal stability of the hybrids formed by the modified PNAs with cDNA (**DNA 1**) and cRNA (**RNA 1**) were determined using temperature dependent UV spectroscopy.

Thermal stability of PNA:DNA and PNA:RNA duplexes

The control **PNA 1** and triantennary GalNAc₃-**PNA 2** and $[C^{\gamma}(S)\text{-GalNAc-T}]_3$ -**PNA 3** were hybridized with **DNA 1** and **RNA 1** to generate corresponding antiparallel PNA:DNA/RNA duplexes (Figure 4). The effect of conjugation of GalNAc on the thermal stability of derived PNA:DNA hybrids was investigated by temperature dependent UV absorbance experiments (Figure 4). All PNA:DNA and PNA:RNA hybrids showed well defined sigmoidal transition suggesting successful formation of duplexes. The DNA duplex of unmodified *aeg*-PNA (**PNA 1:DNA 1**) showed a melting (T_m) of 48.9 °C, while the T_m of GalNAc conjugated **PNA 2:DNA 1** duplexes were slightly higher: triantennary GalNAc₃-**PNA 2:DNA 1** duplex T_m of 52.5 °C and $[C^{\gamma}(S)\text{-GalNAc-T}]_3$ -**PNA 3:DNA 1** duplex T_m ~51.3 °C. Thus, conjugation of GalNAc to PNA showed slight stabilization of corresponding DNA duplexes by 3.6 °C and 2.4 °C, respectively (Table 2), with triantennary duplex being slightly more stable than mono-GalNAc PNA duplexes.

In comparison, the T_m of duplex **PNA 1:RNA 1** from unmodified *aeg*-PNA was 59.5 °C, the T_m of triantennary GalNAc₃-**PNA 2:RNA 1** duplex was 55.8 °C and the T_m of $[C^{\gamma}(S)\text{-GalNAc-T}]_3$ -**PNA 3:RNA 1** duplex was 53.8 °C (Figure 4). Thus, GalNAc conjugated PNAs showed a slight destabilization ($\Delta T_m \sim 4\text{-}6$ °C) of their duplexes with RNA over that of control PNA:RNA duplex. The PNA:RNA duplexes were slightly more stable ($\Delta T_m \sim +2\text{-}3$ °C) than the corresponding PNA:DNA duplexes. The destabilization of PNA:RNA hybrids induced by GalNAc₃ modification was only marginal ($\Delta T_m \sim -1$ to -2 °C/modification) and the melting temperatures were still higher than the corresponding PNA:DNA hybrids.

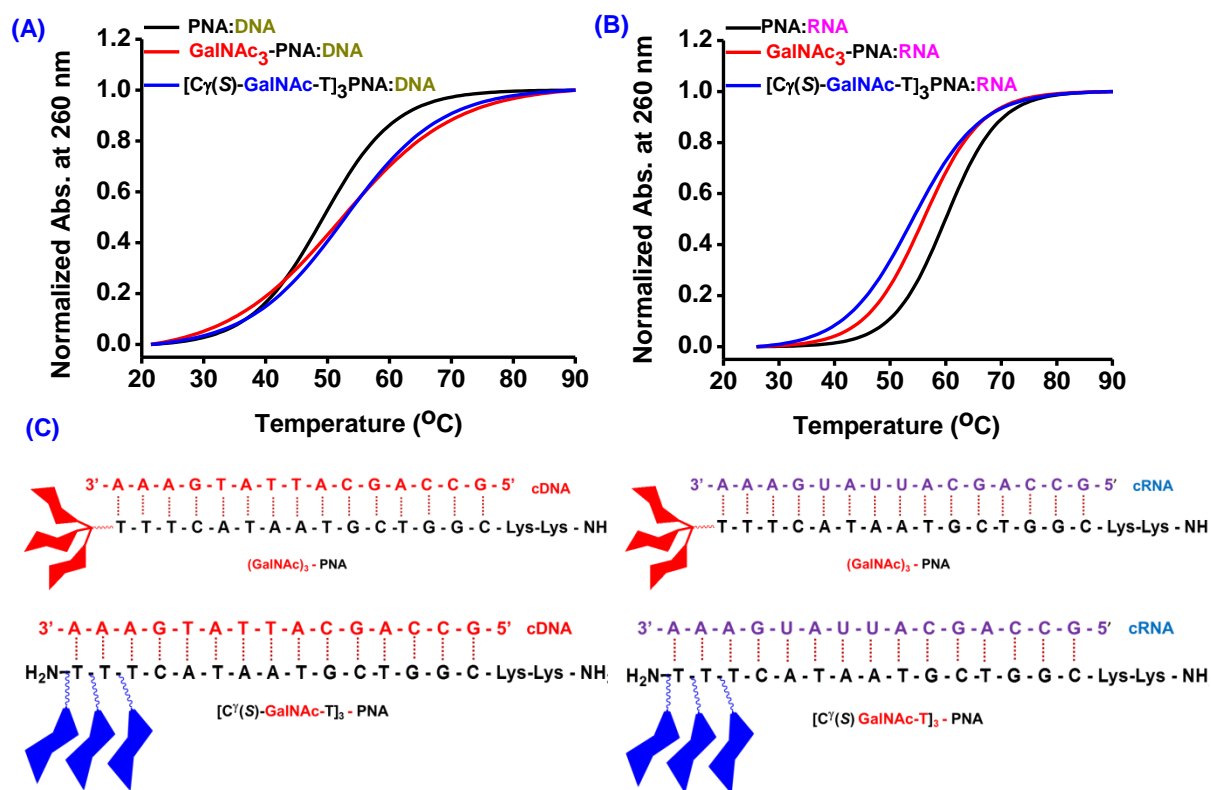


Figure 4. Thermal melting curves for unmodified **PNA 1**, branched GalNAc₃-conjugated **PNA 2**, and sequential GalNAc-conjugated **PNA 3** hybridized to (A) DNA or (B) RNA and (C) Structures of PNA:DNA duplexes. Buffer: 10 mM sodium cacodylate, pH 7.2, NaCl 10 mM. Concentration of PNA and DNA 3 μM of each strand

Table 2. UV-*T_m* values of complementary PNA:DNA duplexes with triantennary-GalNAc₃ PNA and trivalent [C^γ(S)GalNAc-T]₃-PNA units

Entry	PNA Sequence	DNA 1		RNA 1	
		<i>T_m</i>	Δ <i>T_m</i>	<i>T_m</i>	Δ <i>T_m</i>
1	PNA 1 H-TTTCATAATGCTGGC-Lys-Lys-NH ₂	48.9	-	59.5	
2	PNA 2 GalNAc ₃ -TTTCATAATGCTGGC-Lys-Lys-NH ₂	52.5	+ 3.4	55.8	-3.7
3	PNA 3 [C ^γ (S)GalNAc-T] ₃ -CATAATGCTGGC-Lys-Lys-NH ₂	51.3	+ 2.4	53.8	-5.7

Buffer: 10 mM sodium cacodylate, pH =7.2, NaCl 10 mM. *T_m*s are accurate to within ± 0.5 °C

CD studies of PNA:DNA and PNA:RNA duplexes

The effect of conjugation of triantennary GalNAc₃ to N-terminus of PNA or monomeric GalNAc substituted at C^γ in the side chain of PNA backbone on the conformation of derived PNA:DNA/RNA duplexes was studied by CD spectroscopy. The CD-spectra for ss **PNA 1**, and GalNAc conjugated **PNA 2** and **PNA 3** did not show any significant CD bands (SI). The chiral induction from GalNAc₃ substituents on PNA stacking or conformation is negligible. The CD spectra of single stranded DNA and RNA show low intensity positive bands in the region of 260 to 280 nm.

The CD-spectra of duplexes **PNA 1:DNA 1**, **GalNAc₃-PNA 2:DNA 1** and **[C^γ(S)-GalNAc-T]₃-PNA 3:DNA 1** showed almost similar characteristics with weak positive bands at 222 nm, strong positive band at 275 nm and a weak negative band at 250 nm (Figure 5A). In case of corresponding RNA duplexes, positive band at 220 nm was relatively strong, accompanied by strong positive band at 265 nm and weak negative band at 245 nm (Figure 5B). The almost identical CD profiles of the control and GalNAc conjugated PNA:DNA duplexes and similar profile of control and GalNAc conjugated PNA:RNA duplexes suggested that GalNAc modifications do not alter the PNA:DNA/RNA duplex conformation and retain the same as unsubstituted PNA:DNA/RNA duplexes.

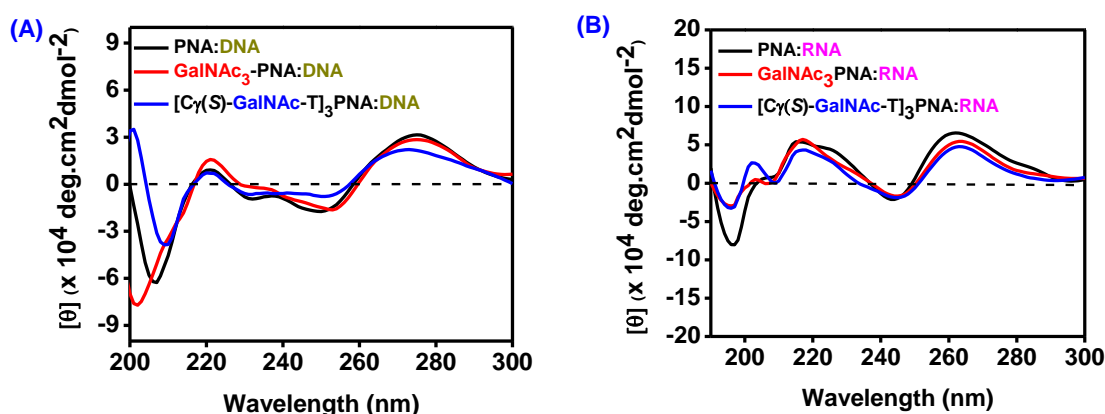


Figure 5. Circular dichroism spectra of (A) PNA:DNA duplexes and (B) PNA:RNA duplexes formed by unmodified **PNA 1**, branched GalNAc-conjugated **PNA 2**, and sequential GalNAc-conjugated **PNA 3**. Buffer: 10 mM sodium cacodylate, pH 7.2, NaCl 10 mM. Concentration of PNA and DNA 5 μ M of each strand.

Cell uptake studies

The cell uptake studies were conducted with fluorescent PNA oligomers *Cf*-PNA 4, *Cf*-GalNAc₃-PNA 5 and *Cf*-[C^γ(S)-GalNAc-T]₃-PNA 6. The fluorescent PNAs upon excitation at 484 nm showed the emission spectra with maximum at 520 nm. The fluorescent intensities of duplexes were slightly lower than that of single-stranded fluorescently labeled PNAs when excited at either at 458 nm or 484 nm. The GalNAc conjugated PNAs (**PNA 2** and **PNA 3**) were designed for selective uptake by hepatocytes (HepG2 cells) that have ASGPR on the cell surfaces, which bind to triantennary GalNAc₃. HepG2 cells were treated with 5(6)-carboxyfluorescein tagged *Cf*-GalNAc₃-PNA 5 and *Cf*-[C^γ(S)-GalNAc-T]₃-PNA 6 and their uptake was studied by confocal microscopy. In these experiments, 5(6)-carboxyfluorescein tagged isosequential *aeg*-PNA was used as control. To confirm the selectivity of uptake, the experiments were conducted with HEK-293 cells, which lack ASGPR, as negative control.⁸

1
2
3 **Cell uptake studies with HepG2 cells.** HepG2 cells were grown in MEM medium at 37°C
4 under 5% CO₂ to reach a confluency of 50%. They were then treated with 5(6)-
5 carboxyfluorescein functionalized PNAs *Cf*-GalNAc₃-**PNA 5**, *Cf*-[C^γ(S)-GalNAc-T]₃-**PNA 6**
6 or unmodified control *Cf*-**PNA 4** each at 4 μM concentrations. The internalized PNAs were
7 visualized by imaging the cells with confocal laser scanning microscopy (Figure 6). To stain
8 the nucleus, 4' 6-diamidino-2-phenylindole (DAPI) was used. Figures 6A-C show the overlay
9 of the images from the DAPI and carboxyfluorescein channels. The fluorescence images were
10 merged with the corresponding differential interference contrast (DIC) images to confirm that
11 the peptides were within the cell boundaries (Figures 6D-F).
12
13
14
15
16
17
18

19
20 In case of cells treated with *Cf*-GalNAc₃-**PNA 5** or *Cf*-[C^γ(S)-GalNAc-T]₃-**PNA 6**, the
21 presence of green fluorescence indicated that the PNAs were taken up by HepG2 cells. This is
22 evident from Figures 6B and 6E, which show the nuclei and the cell boundary along with green
23 puncta that appear within the cells. A comparison of the fluorescence intensity and the number
24 of cells that show PNA uptake indicated that the extent of internalization of *Cf*-[C^γ(S)-GalNAc-
25 T]₃-**PNA 6** with three monovalent GalNAc substitutions was higher than that of triantennary *Cf*-
26 GalNAc₃-**PNA 5**. The localization of *Cf*-[C^γ(S)-GalNAc-T]₃-**PNA 6** within the cell was clearly
27 observed as punctate of green fluorescence in Figure 6D. The appearance of discrete punctate
28 in the vicinity of the nucleus and distributed throughout the cell suggested that the
29 internalization could be a result of endocytosis, as expected for ASGPR mediated cellular
30 uptake. In contrast to the GalNAc modified PNAs, the unmodified *Cf*-**PNA 4** did not show any
31 green fluorescence (Figure 6E and 6F) in the cells, indicating no internalization. These results
32 showed that the cell penetrating ability of the GalNAc₃ modified PNAs (**PNA 5** and **PNA 6**)
33 was indeed conferred by the GalNAc₃ functionalization.
34
35
36
37
38
39
40
41
42
43
44
45
46
47
48
49
50
51
52
53
54
55
56
57
58
59
60

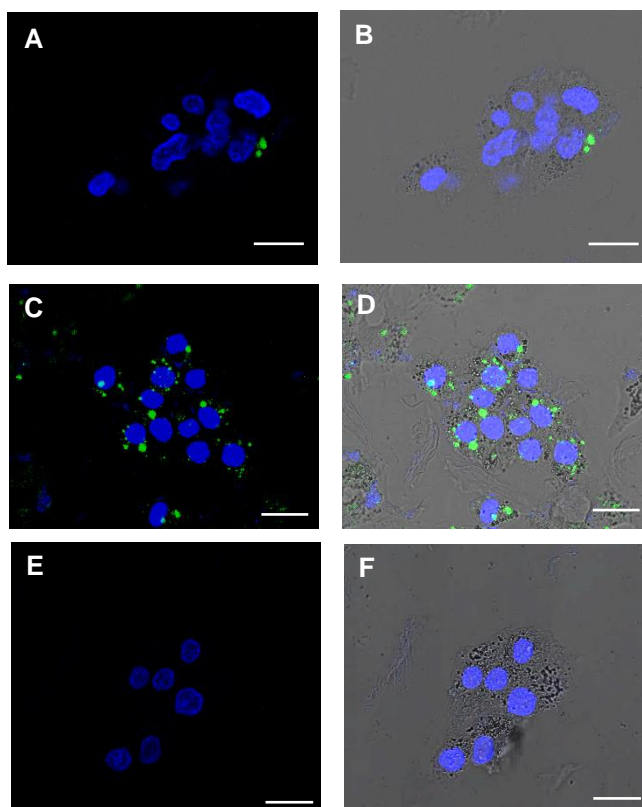


Figure 6. Confocal microscopy images of HepG2 cells treated with *Cf*-GalNAc₃-**PNA 5** (A-B), and *Cf*-[C^γ(*S*)-GalNAc-T]₃-**PNA 6** (C-D) and *Cf*-**PNA 4** (E-F). A, C, and E are merged images of DAPI and carboxyfluorescein channels. B, D, and F show merged images from the DAPI and carboxyfluorescein channels along with differential interference contrast image showing the intact cells (gray), nuclei (blue), and internalized PNAs (green). Scale bars represent 25 μm.

Cellular uptake studies with HEK-293 cells. The HEK-293 cells in which ASGPR are not expressed were used as negative controls to confirm that observed internalization of GalNAc₃ modified PNAs was indeed mediated by specific interactions with the cell surface receptor ASGPR. The cells were then treated with *Cf*-GalNAc₃-**PNA 5**, *Cf*[C^γ(*S*)-GalNAc-T]₃-**PNA 6** or unmodified *Cf*-**PNA 4** at same concentrations (4 μM) and experimental conditions as in the experiment with HepG2 cells, followed by imaging under confocal laser scanning microscopy (Figure 7). The panels, A, D, and G correspond to the DAPI signals indicating the nuclei of the cells. The panels, B, E, and H show the images obtained from the detector capturing carboxyfluorescein emission signals. The panels C, F and I show the merged images of the DAPI and carboxyfluorescein channels along with the respective DIC image.

In case of *Cf*-GalNAc₃-**PNA 5** treated cells, no green fluorescence emission was observed. This is evident from Figure 7C, which shows the nuclei and the cell boundary but no PNA within the cells. Similar results were obtained with *Cf*[C^γ(*S*)-GalNAc-T]₃-**PNA 6** and

unmodified *Cf*-PNA 4 as well. These results clearly indicate that PNAs, with or without GalNAc modifications, are incapable of cell penetration into HEK 293 cells.

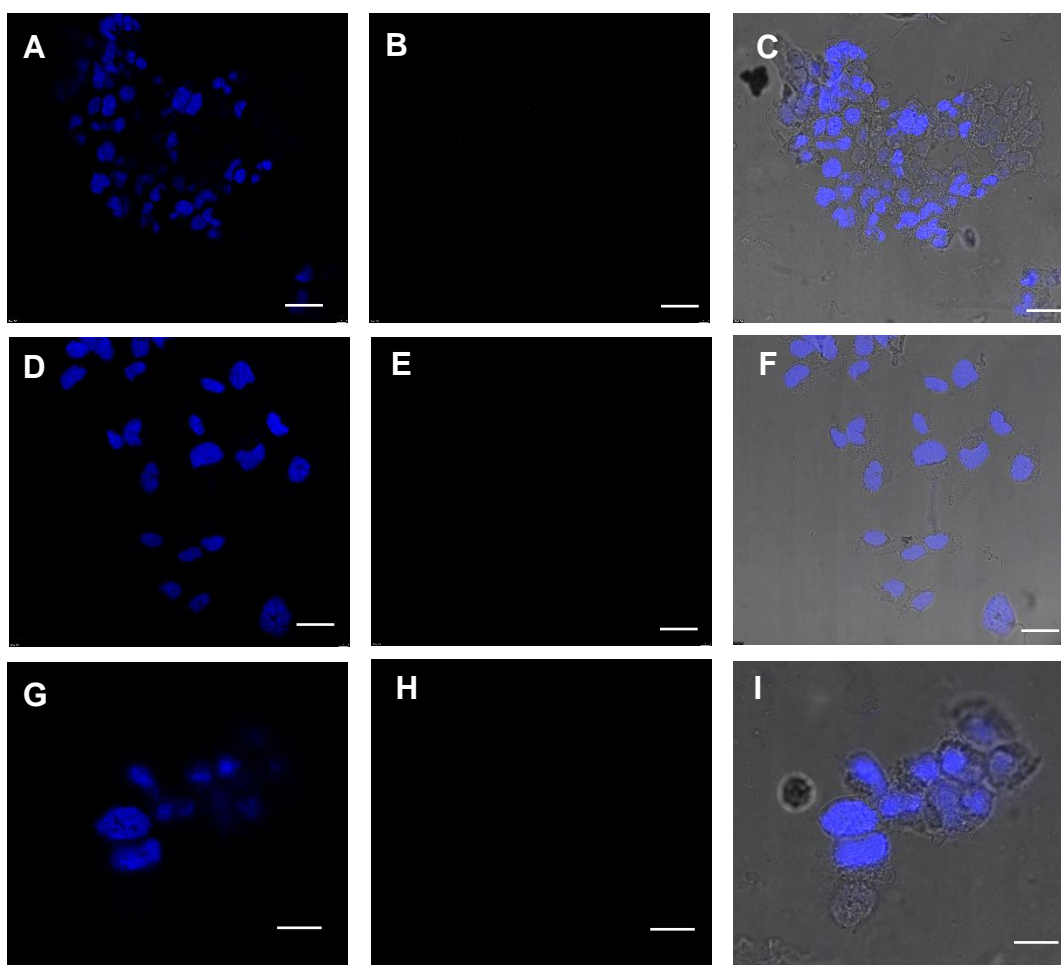


Figure 7. Confocal microscopy images of HEK-293 cells treated with *Cf*-GalNAc₃-PNA 5 (A-C), *Cf*[C γ (S)-GalNAc-T]₃-PNA 6 (D-F) and *Cf*-PNA 4 (G-I). A, D, and G are images of DAPI. B, E, and H show signals from carboxyfluorescein channel. C, F, and I show the merged image of DAPI channels and carboxyfluorescein channels along with differential interference contrast image showing the intact cells (grey), nuclei (blue), and internalized PNAs (green). Scale bars represent 25 μ m.

Flow cytometry studies. For quantitative comparison of the uptake of the GalNAc modified PNAs by HepG2 cells flow cytometry studies were carried out. HepG2 cells were cultured as mentioned above. The cells were treated with 5(6)-carboxyfluorescein functionalized PNAs *Cf*-GalNAc₃-PNA 5, *Cf*[C γ (S)-GalNAc-T]₃-PNA 6 or unmodified control *Cf*-PNA 4 each at 4 μ M concentrations for 12 hours. The results show cells treated with GalNAc modified PNAs showed significant uptake as compared to untreated cells and cells incubated with unmodified control *Cf*-PNA 4 (Figure 8). Similar to the results of the confocal microscopy studies, the cells were found to internalize *Cf*[C γ (S)-GalNAc-T]₃-PNA 6 more than *Cf*-GalNAc₃-PNA 5. While

the measured uptake was only 3.1% for triantennary *Cf*-GalNAc₃-**PNA 5**, it was 39.5% for the *Cf*[C^γ(*S*)-GalNAc-T]₃-**PNA 6**. Thus, conjugation of three GalNAc moieties to the last three PNA monomeric residues at the N terminus was found to effect a 12.7 fold increase in the uptake of the PNA by HepG2 cells compared to the triantennary GalNAc modification.

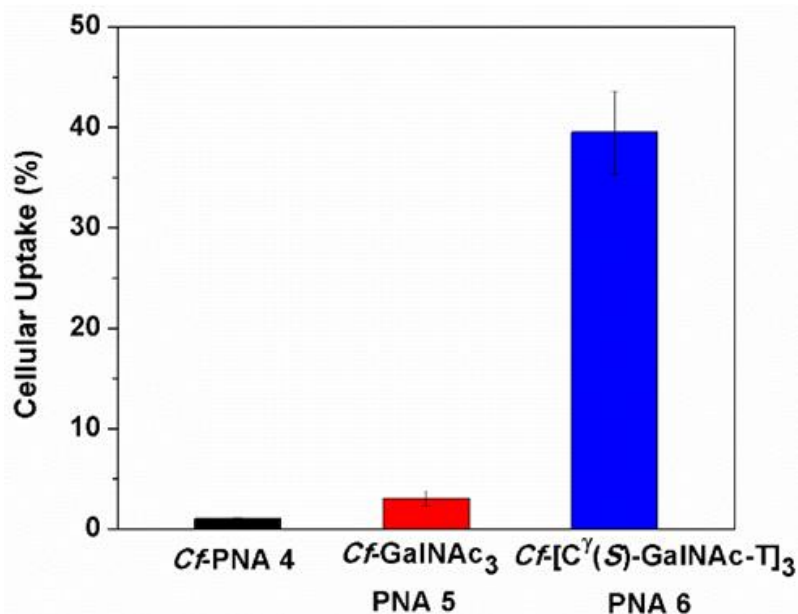


Figure 8. Uptake of unmodified control *Cf*-**PNA 4**, *Cf*-GalNAc₃-**PNA 5**, and *Cf*[C^γ(*S*)-GalNAc-T]₃-**PNA 6** by HepG2 cells as measured by flow cytometry. The results shown are average of two independent measurements. The error bars represent standard deviations. The percentage refers to the fraction of total number of cells that are fluorescent among the total number of cells analysed by FACS in each case.

Cytotoxicity studies. For ultimate therapeutic application of the GalNAc modified PNAs, it is essential to confirm whether the modified PNAs elicit any adverse effects in the target cells. We assessed the cytotoxicity of the GalNAc modified PNAs GalNAc₃-**PNA 2** and [C^γ(*S*)-GalNAc-T]₃-**PNA 3** towards HepG2 cells and compared them with the unmodified control **PNA 1** using 3-(4,5-dimethylthiazol-2-yl)-2,5-diphenyltetrazolium bromide (MTT) assay (Figure 9). The cells were incubated with PNAs at the concentration of 4 μM for 12 hours, as in the cellular uptake studies, prior to treatment with MTT. The results show that the viability of the cells were not significantly altered by the treatment of the cells with the PNAs. The viability of the cells were marginally reduced when they were treated with GalNAc₃-**PNA 2**, while treatment with [C^γ(*S*)-GalNAc-T]₃-**PNA 3** did not lead to any reduction in the viability compared to the control PNA. On the contrary, treatment of the cells with [C^γ(*S*)-GalNAc-T]₃-**PNA 3** slightly enhanced the cell viability compared to the control and untreated PNAs; however, this effect was not significant.

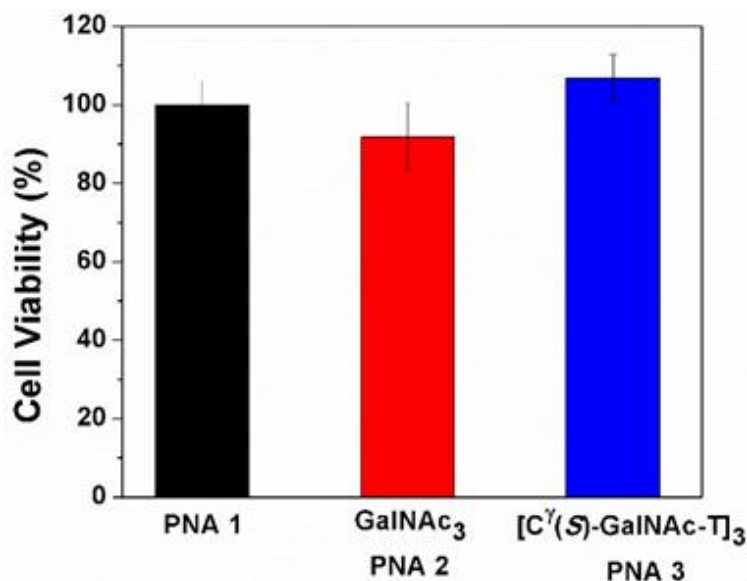


Figure 9. Cell viability measured using 3-(4,5-dimethylthiazol-2-yl)-2,5-diphenyltetrazolium bromide (MTT) assay for HepG2 cells after treatment with 4 μ M of **PNA 1**, GalNAc₃-**PNA 2** or [C^γ(S)-GalNAc-T]₃-**PNA 3** for 12 hours. The data shown are average of three measurements. The error bars represent standard deviations.

Discussion

From detailed structure-activity relationship studies on oligonucleotide-GalNAc conjugates²⁸ it was found that the branched triantennary (GalNAc)₃ moiety linked to siRNA through spacer chain as depicted in Figure 1 was the best in terms of its binding to the ASGPR. This is perhaps due to the fact that this cluster displays the appropriate inter-GalNAc distance and cluster geometry to match the receptor binding site.²⁹⁻³³ The siRNA conjugates in which the GalNAc moieties are linearly displayed with conjugation on successive bases, ribosugars, acyclic and cyclic linkers or to phosphate groups on backbone in a sequence rather than in cluster have also been examined.^{33,34} It was found that conjugates having sequential GalNAc moiety linked to ribosugars or bases were as good in potency as the branched triantennary GalNAc₃ linked siRNAs.³⁵ In the only report so far on PNA-GalNAc conjugate, wherein the two GalNAc units are linked via lysine at N-terminus to PNA, it was found that the bioactivity and distribution of the PNA conjugate was better than the unconjugated PNA.^{20,21} In this context, the present comparative results show that the linear PNA conjugate with three monovalent GalNAc ligands linked to successive C^γ site of *aeg* PNA backbone (**PNA 3**) shows 40 times times more internalization in HepG2 cells than the unconjugated PNA and 13 times more uptake than the N-terminus branched GalNAc₃ conjugate (**PNA 2**). These PNAs are not internalized in HEK293 cells that lack the ASGP receptor and hence the GalNAc induced enhancements in cell uptake of linear conjugates are significant and interesting. It may be

1
2
3 pointed out that the relative enhancement in internalization of linear vs branched GalNAc-PNA
4 conjugates is much higher than that between the corresponding GalNAc-siRNA conjugates.
5 This suggests that PNA conformation provides a favourable display geometry for the linearly
6 distributed GalNAc units on PNA backbone compared to the N-terminus cluster for recognition
7 of the ASGPR. The binding of linear PNA conjugate **PNA 3** may also be assisted by some non-
8 specific interaction of hydrophobic PNA strand with the receptor facilitating a favourable
9 orientation for binding with the receptor, a feature that is perhaps not possible in **PNA 2** where
10 the N-terminus branched (GalNAc)₃ cluster is far removed from PNA chain. Further
11 understanding requires a study evaluating the binding affinities of PNA conjugates with the
12 receptor.
13
14
15
16
17
18
19
20

21 **Conclusions**

22
23
24 Motivated by GalNAc₃-conjugated oligonucleotide drugs that are efficiently taken up by
25 liver cells and by the approval of givosiran (GIVLAARI[®]), PNA was conjugated with GalNAc
26 in two different ways: (i) a triantennary branched structure linked at the N-terminus of the PNA
27 via a spacer chain and (ii) a sequential architecture in which three monovalent GalNAc units
28 were conjugated at the C_γ of the backbone on three successive N-terminal PNA residues. Both
29 type of GalNAc-conjugated PNAs formed stable duplexes with complementary DNA with
30 thermal stability enhanced compared to unmodified PNA, and both had slightly lower stability
31 with complementary RNA than the unmodified PNA. The CD spectral profiles showed that
32 conjugation of the bulky branched GalNAc₃ or of the three successive GalNAc-linked residues
33 did not alter the conformations of duplexes formed with DNA or RNA relative to the duplexes
34 formed with the unconjugated PNA. The GalNAc-conjugated PNAs were fluorescently labeled
35 with carboxyfluorescein for cell permeability studies. The PNA with three sequential
36 monovalent GalNAc units was more efficiently taken up by HepG2 cells, which express the
37 ASGPR, than either the GalNAc₃-PNA conjugate or the unmodified PNA. None of the PNAs
38 were efficiently internalized by HEK293 cells, which do not express the receptor. These results
39 indicate that in the case of PNAs the architecture of the GalNAc conjugation tunes the
40 efficiency of uptake. This is rather significant, as it is not the case for antisense oligonucleotides
41 and siRNAs.³⁴⁻³⁶ On the other hand, the hydrophobic nature of the anionic backbone of
42 antisense oligonucleotide conjugates (phosphodiester vs phosphorothioate) has been shown to
43 affect the receptor binding.³⁶ As PNAs are neutral and in the present work they are slightly net
44 positive due to terminal lysines, the ligand-receptor recognition may get modified which
45
46
47
48
49
50
51
52
53
54
55
56
57
58
59
60

1
2
3 deserves further evaluation. Nevertheless, our data indicate that appropriately designed
4 GalNAc-conjugate PNAs have potential in therapeutic applications.
5
6

7 8 **Experimental Methods** 9

10 The chemicals used were of laboratory or analytical grade. All the solvents used were
11 distilled or dried to carry out different reactions. Reactions were monitored by thin layer
12 chromatography (TLC). Usual workup involved sequential washing of the organic extract with
13 water and brine followed by drying the organic layer over anhydrous sodium sulfate and
14 evaporation of solvent under vacuum. TLCs were carried out on pre-coated silica gel GF₂₅₄
15 sheets (Merck 5554). TLCs were analyzed under UV lamp, by iodine spray and by spraying
16 with ninhydrin solution, followed by heating of the plate. Column chromatographic separations
17 were performed using silica gel (60-120 or 100-200 mesh). The scheme for synthesis of
18 Compound **1** is shown in Supporting Information (Scheme 4, S4) following reported
19 procedures.^{6,7,22} Compounds **34** and **1** were characterized using ¹H, ¹³C NMR and mass spectral
20 data (Supporting Information).
21
22
23
24
25
26
27
28
29

30 ¹H and ¹³C NMR spectra were recorded using JEOL 400 MHz NMR spectrometer (400
31 MHz for ¹H and 100 MHz for ¹³C). The delta (δ) values for chemical shifts are reported in ppm
32 and are referred to internal standard TMS or deuterated NMR solvents. ¹³C NMR were
33 recorded using broad band ¹H decoupling conditions ¹³C{¹H}. The optical rotation values were
34 obtained on Rudolph Research Analytical Autopol V polarimeter. Mass spectra for reaction
35 intermediates were obtained by Applied Biosystems 4800 Plus MALDI-TOF/TOF mass
36 spectrometry using TiO₂ or 2,5-dihydroxybenzoic acid (DHB) and the integrity of PNA
37 oligomer was checked on the same instrument using SA, DHB or CHCA as matrix. High
38 resolution mass spectra for final PNA GalNAc₃ and [C^γ(S)-GalNAc-T]₃ were recorded on
39 Synapt G2 High Definition Mass Spectrometry. PNA oligomers were purified on Agilent
40 technologies 260 infinity HPLC system using semi-preparative BEH130 C18 (10 x 250 mm)
41 column. The unmodified PNA monomers were obtained from ASM technologies Ltd.
42 Germany. The complementary DNA and RNA oligonucleotides were obtained commercially
43 from Integrated DNA Technologies (IDT). Salts and reagents used in buffer preparation such
44 as NaCl, sodium cacodylate etc. were obtained from Sigma-Aldrich. The pH of the buffer
45 solutions was adjusted using NaOH or HCl, from Sigma Aldrich.
46
47
48
49
50
51
52
53
54
55
56
57
58
59
60

N*-(Decanoic)-tris-[(carboxyethoxymethyl)aminopropyl]-tri(*O*-acetyl) *N*(acetyl galactosamine)aminomethane [(Fmoc)methoxy]carbonyl]-benzyl lysinate **1b*

To a solution of [$N^{\text{O}}\text{H}(\text{Boc}), N^{\text{O}}\text{H}(\text{Fmoc})$]-lysine benzyl ester (0.5 g, 0.25 mmol) in DMF (2 mL) were added HBTU (0.3 g, 0.76 mmol) and DIEA (0.14 mL, 0.92 mmol) and the resulting mixture was stirred for few minutes. A solution of compound **1a** (0.42 g, 0.76 mmol) in DMF (2 mL) was added, and stirring was continued at room temperature overnight. Solvents and volatiles were removed under reduced pressure, and the residue was dissolved in DCM (20 mL), washed with saturated NaHCO_3 (5 mL) and water (5 mL). After drying over anhydrous Na_2SO_4 the solvent was evaporated under reduced pressure. The residue was purified by silica gel chromatography (eluent: 3-15% MeOH in DCM) to obtain compound **1b** (0.6 g, 50%). ^1H NMR (400 MHz, $\text{DMSO}-d_6$) δ 7.91 – 7.69 (m, 14H), 7.44 – 7.28 (m, 8H), 6.99 (s, 1H), 5.75 (s, 1H), 5.21 (d, $J = 3.4$ Hz, 2H), 5.12 (s, 1H), 4.97 (dd, $J = 11.2, 3.4$ Hz, 2H), 4.49 (d, $J = 8.5$ Hz, 2H), 4.32 – 4.18 (m, 2H), 4.07 – 3.96 (m, 9H), 3.88 (dd, $J = 18.9, 10.0$ Hz, 3H), 3.70 (dt, $J = 10.8, 5.6$ Hz, 3H), 3.55 (m, $J = 12.0, 5.7$ Hz, 12H), 3.44 – 3.36 (m, 4H), 3.07 – 2.96 (m, 13H), 2.28 (t, $J = 6.3$ Hz, 6H), 2.10 (s, 8H), 2.04 (dd, $J = 13.1, 6.2$ Hz, 9H), 1.99 (d, $J = 2.5$ Hz, 9H), 1.89 (s, 8H), 1.77 (s, 8H), 1.55 – 1.40 (m, 22H), 1.33 (s, 1H), 1.24 – 1.16 (m, 9H), 1.10 (s, 2H). $^{13}\text{C}\{^1\text{H}\}$ NMR (101 MHz $\text{DMSO}-d_6$) δ 172.5, 172.3, 172.0, 170.0, 169.9, 169.6, 169.4, 156.2, 143.8, 140.7, 136.0, 128.4, 128.00, 127.6, 127.0, 125.2, 120.1, 115.6, 101.0, 70.5, 69.8, 68.6, 68.3, 67.3, 66.7, 65.8, 64.9, 61.4, 59.5, 54.9, 54.0, 49.4, 46.6, 39.5, 36.4, 36.3, 36.0, 35.1, 29.4, 28.7, 22.8, 21.8, 20.5 ppm. MS (MALDI-TOF) m/z calcd. for $\text{C}_{117}\text{H}_{172}\text{N}_{12}\text{O}_{42}$ [$\text{M}+\text{H}$] $^+$, 2418.70 ; found: 2441.00 [$\text{M}+\text{Na}$] $^+$.

***N*-(decanoic) -tris-[(carboxyethoxymethyl)aminopropyl]-tri(*O*-acetyl) *N*-acetyl galactosamine]aminomethane [(Fmoc)methoxy]carbonyl]-Lysine (**1c**):**

Compound **1b** (0.5 g, 0.22 mmol) was dissolved in methanol, evaporated under reduced pressure to remove traces of chlorinated solvent from previous step, re-dissolved in MeOH, 10 wt% Pd-C (1.0 g, wet Degussa type) was added at 0 °C. The reaction was hydrogenated under normal pressure by maintaining temperature 20-25 °C for 1h. After completion of reaction (monitored by TLC), the reaction content was filtered through celite and washed with MeOH. The combined filtrates were evaporated under reduced pressure to afford **1c** (0.16g, 40%) as a white solid. ^1H NMR (400 MHz, $\text{DMSO}-d_6$) δ 7.90 (t, $J = 7.9$ Hz, 8H), 7.81 (t, $J = 5.5$ Hz, 3H), 7.77 – 7.67 (m, 3H), 7.41 (t, $J = 7.4$ Hz, 2H), 7.32 (t, $J = 7.4$ Hz, 2H), 7.00 (d, $J = 6.0$ Hz, 1H), 5.21 (d, $J = 3.4$ Hz, 3H), 5.00 – 4.94 (m, 3H), 4.50 (d, $J = 8.5$ Hz, 3H), 4.28 – 4.19 (m, 3H), 4.05 – 3.96 (m, 9H), 3.87 (dt, $J = 11.0, 8.9$ Hz, 3H), 3.70 (dt, $J = 10.8, 5.6$ Hz, 3H), 3.53 (dd, $J = 13.6, 7.1$ Hz, 14H), 3.43 – 3.37 (m, 5H), 3.07 – 2.96 (m, 14H), 2.28 (t, $J = 6.3$ Hz, 6H),

2.10 (s, 9H), 2.03 (dd, $J = 13.1, 6.2$ Hz, 10H), 1.99 (s, 10H), 1.88 (s, 9H), 1.77 (s, 9H), 1.49 (dq, $J = 19.4, 6.5$ Hz, 24H), 1.33 (s, 2H), 1.25 – 1.18 (m, 18H). $^{13}\text{C}\{1\text{H}\}$ NMR (101 MHz DMSO- d_6) δ 174.0, 172.5, 172.0, 171.9, 170.0, 169.9, 169.4, 167.0, 155.6, 153.4, 144.0, 143.9, 142.6, 140.7, 140.2, 139.4, 138.9, 137.4, 134.1, 131.7, 128.9, 127.6, 127.1, 125.2, 123.2, 122.7, 121.4, 120.0, 115.6, 114.6, 109.8, 101.0, 70.5, 69.8, 68.6, 68.2, 67.3, 66.7, 65.4, 61.4, 59.5, 39.5, 36.3, 35.8, 35.0, 31.5, 31.3, 29.4, 28.7, 25.30, 22.8, 22.0, 21.8, 20.5, 13.9, 10.8 ppm. MS (MALDI-TOF) m/z calcd. for $\text{C}_{110}\text{H}_{166}\text{N}_{12}\text{O}_{42} [\text{M}+\text{H}]^+$, 2328.58 ; found: 2351.57 $[\text{M}+\text{Na}]^+$.

$\text{N}^{\alpha}\text{H}[(\text{Fmoc})-\text{N}^{\omega}\text{H}(\text{Boc})-\text{N},\text{N}$ methoxymethyl lysine amide (4)

To a stirring solution of Fmoc-protected Boc Lysine **3** in (5 g, 10.7 mmol) CH_2Cl_2 (50 ml) was added EDC (1.8 g, 11.8 mmol) and HOBt (2 g, 13 mmol). After stirring for 10 min at 23 °C, N,O -dimethylhydroxylamine hydrochloride (1.2 g, 12 mmol) in EtPr_2N (3 ml, 24 mmol) was added and the reaction mixture was stirred 12 h. It was diluted with EtOAc and washed aq. HCl (0.1 N), 10% aq. K_2CO_3 , dried over anhydrous MgSO_4 and concentrated. The residue obtained was purified on silica gel (100–200 mesh) using petroleum ether and EtOAc to give compound **4** as a white powder (4.5 g, 80%). ^1H NMR (400 MHz, CDCl_3) δ 7.75 (d, $J = 8.1$ Hz, 2H), 7.60 (t, $J = 6.6$ Hz, 2H), 7.39 (t, $J = 7.5$ Hz, 2H), 7.33 – 7.28 (m, 2H), 5.61 (d, $J = 8.9$ Hz, 1H), 4.68 (d, $J = 49.4$ Hz, 2H), 4.36 (d, $J = 7.2$ Hz, 2H), 4.21 (t, $J = 7.0$ Hz, 2H), 3.76 (s, 3H), 3.21 (s, 3H), 3.11 (d, $J = 4.5$ Hz, 2H), 1.92 (s, 1H), 1.76 (td, $J = 13.4, 7.6$ Hz, 1H), 1.61 (dd, $J = 13.9, 5.5$ Hz, 2H), 1.51 (dd, $J = 14.7, 7.5$ Hz, 2H), 1.42 (s, 9H), 1.28 – 1.18 (m, 2H). $^{13}\text{C}\{1\text{H}\}$ NMR (101 MHz, CDCl_3) δ 172.5, 156.0, 155.8, 143.7, 143.5, 141.0, 127.4, 126.8, 124.9, 119.5, 78.9, 77.1, 67.0, 61.4, 50.5, 46.9, 40.0, 32.2, 31.8, 29.3, 28.2, 22.2, 20.8 ppm. HRMS (ESI-TOF) m/z calcd. For $\text{C}_{28}\text{H}_{37}\text{N}_3\text{O}_6$: 511.2682 and found 534.2571 $[\text{M}+\text{Na}]^+$.

$\text{N}^{\omega}\text{H}(\text{Boc}),\text{N}^{\alpha}\text{H}[(\text{Fmoc})$ pentanaldehyde (5)

Compound **4** (3 g, 6 mmol) was dissolved in THF (15ml), cooled to -20°C , and LiAlH_4 (0.2 gm, 5.2 mmol) was added slowly. After 1h, the reaction was quenched with EtOAc and the organic layer washed with aq. HCl (0.1N), dried over MgSO_4 and concentrated. The residue obtained was purified on silica gel (100–200 mesh) using petroleum ether and EtOAc to give compound **5** as a pale yellow oil (2.6 g, 95 %). ^1H NMR (400 MHz, DMSO- d_6) δ 7.39 – 7.27 (m, 5H), 7.24 (m, $J = 5.2$ Hz, 1H), 7.19 (m, $J = 5.9$ Hz, 1H), 6.70 (m, $J = 8.7$ Hz, 1H), 5.00 (d, $J = 5.2$ Hz, 2H), 4.75 (d, $J = 16.8$ Hz, 2H), 4.4 (d, $J = 16.7$ Hz, 2H), 4.20 (dd, $J = 33.7, 18.8$ Hz, 1H), 3.95 (dd, $J = 44.8, 17.4$ Hz, 1H), 3.81 – 3.70 (m, 1H), 3.49 – 3.18 (m, 4H), 3.05 (dd, $J = 19.4, 7.5$ Hz, 2H), 1.75 (d, $J = 1.8$ Hz, 2H), 1.64–1.47 (m, 2H), 1.36 (s, 9H). $^{13}\text{C}\{1\text{H}\}$ NMR (101 MHz, CDCl_3) δ 199.5, 156.3, 143.9, 141.5, 127.9, 127.2, 125.2, 120.1, 79.4, 77.1, 67.1,

60.2, 47.3, 39.9, 29.9, 28.6, 28.5, 22.2 ppm. HRMS (ESI-TOF) m/z calcd. For $C_{28}H_{37}N_3O_6$ 452.2311 and found 452.5510[M+H]⁺.

N-[ethylamino(NHFmoc)-C^γ(S)(NHBoc)aminobutyl] benzyl glycinate (7)

To a solution of the aldehyde **5** in ethanol, benzyl glycine ester hydrochloride (3 g, 66 mmol) was added DIPEA and neutralized with (0.5 mL, 40 mmol) at ice cold condition, stirred for 5-10 min, followed by addition of sodium cyanoborohydride (1.7 g, 26 mmol) with continued stirring for 4 h. After completion of reaction (monitored by TLC), solvent was evaporated and the product was extracted with EtOAc. The organic layer was concentrated, subjected to column chromatography purification, and the product was eluted with 35% EtOAc: Pet-ether to obtain compound **7**. Yield (1.5 g, 37%). ¹H NMR (400 MHz, CDCl₃) δ 7.75 (d, $J = 7.5$ Hz, 2H), 7.61 (d, $J = 7.1$ Hz, 6H), 7.41 – 7.27 (m, 2H), 5.15 (t, $J = 6.8$ Hz, 2H), 4.60 (s, 1H), 4.41 (d, $J = 6.4$ Hz, 1H), 4.21 (t, $J = 6.7$ Hz, 2H), 3.69 (s, 1H), 3.45 (q, $J = 17.5$ Hz, 2H), 3.10 (d, $J = 4.9$ Hz, 1H), 2.67 (dd, $J = 12.5, 4.5$ Hz, 1H), 1.54 – 1.29 (m, 13H), 1.28 – 1.18 (m, 2H). ¹³C{¹H} NMR (101 MHz, CDCl₃) δ 173.6, 156.5, 144.2, 141.5, 128.9, 127.7, 127.1, 125.2, 121.14, 120.1, 108.1, 77.2, 66.8, 66.6, 53.5, 53.0, 52.0, 50.9, 49.7, 47.9, 47.5, 34.2, 28.6, 23.0, 22.5, 22.4 ppm. HRMS (ESI-TOF) m/z calcd. For $C_{35}H_{43}N_3O_6$ 601.3152 and found 601.7440 [M+H]⁺.

N-[ethylamino(NH(Fmoc)-C^γ(S)butylamino(NHBoc)]-N[acetamido(N1-thyminy)] benzyl glycinate (9)

To thymine acetic acid **8** (1 g, 55 mmol) in anhydrous DMF (4 mL), the amine **7** (5 g, 80 mmol) was added and cooled to 0 °C. After 5 min stirring, HBTU (3 g, 81.5 mmol) and DIPEA (1.5 mL, 12 mmol) were added to the reaction mixture and stirred for 12 h at RT. After completion of reaction, it was poured into water (25 ml), neutralized with *sat.aq.* KHSO₄ (10 mL), and extracted with ethyl acetate (3 x 20 mL). The organic layer was dried over anhydrous Na₂SO₄. The solvent was removed under reduced pressure and product was purified by column chromatography, eluting with petroleum ether/EtOAc (1:1) to obtain the compound **9**. (Yield 2.8 g, 47%). ¹H NMR (400 MHz, CDCl₃) δ 9.06 (d, $J = 51.6$ Hz, 1H), 7.73 – 7.25 (m, 13H), 6.78 (t, $J = 54.4$ Hz, 1H), 5.52 (d, $J = 8.0$ Hz, 1H), 5.21 – 4.97 (m, 2H), 4.74 – 4.45 (m, 2H), 4.41 – 3.96 (m, 4H), 3.86 – 3.66 (m, 2H), 3.43 (dd, $J = 25.6, 5.1$ Hz, 2H), 3.14 – 2.75 (m, 3H), 1.80 (t, $J = 7.4$ Hz, 3H), 1.42 (d, $J = 18.8$ Hz, 12H), 1.24 (s, 2H). ¹³C{¹H} NMR (101 MHz, CDCl₃) δ 169.3, 169.1, 168.4, 168.0, 164.4, 156.7, 156.5, 156.3, 152.1, 151.54 151.3, 144.1, 144.0, 143.9, 143.8, 141.5, 141.3, 141.1, 135.2, 134.9, 129.0, 128.9, 128.8, 128.6, 128.4, 127.8, 127.8, 127.2, 125.3, 120.1, 110.9, 79.3, 77.2, 68.0, 67.4, 66.8, 66.5, 66.3, 50.5, 50.0, 49.4, 48.2,

1
2
3 47.4, 47.2, 40.1, 39.9, 31.9, 31.5, 29.7, 28.5, 23.0, 22.9, 12.3. HRMS (ESI-TOF) m/z calcd.
4 For $C_{42}H_{49}N_5O_9$ 767.3530 and found 768.3619 $[M+H]^+$.

5
6
7 ***N*-[ethylamino(NH(Fmoc)-*C* γ (*S*))butylamine]-*N*[acetamido(*N*1-thyminy)] benzyl
8 **glycinate (10)**
9**

10
11 Compound **9** (2 g, 2.8 mmol) was dissolved in DCM (75 mL) along with trifluoroacetic
12 acid (15 mL) and the reaction was stirred at room temperature for 30 minutes. The reaction
13 mixture was diluted with toluene (100 mL) and concentrated under reduced pressure. The
14 mixture was diluted with toluene (100 mL) and concentrated under reduced pressure. The
15 residue was co-evaporated with toluene (2 x 100 mL) and dried under reduced pressure using
16 a high vacuum pump to yield **10** as the TFA salt (1.7 g) which was used for the next reaction
17 without any further purification. HRMS [ESI-TOF] m/z calculated for $C_{37}H_{41}N_5O_7$. 667.3006;
18 Found 690.1689 $[M+Na]^+$.

19
20
21
22
23
24 ***N*-ethylamino(NHFmoc)-*C* γ (*S*)[(2-*N*-acetyl galactosamino-3,4,6-tri-*O*-acetyl-1-*O*-
25 **butylcarboxy)amidobutyl]-*N*-[acetamido-*N*1-thyminy)]benzyl glycinate (12)**
26
27**

28 To a solution of tri-*O*-acetyl-*N*(acetyl)-galactosamine pentanoic acid **11** (1.6 g, 3.5
29 mmol) in DMF (2 mL) were added HBTU (2 g, 5 mmol) and DIEA (1 mL, 7.3 mmol). The
30 resulting mixture was stirred for few minutes. A solution of compound **10** (3.5 g, 5.1 mmol) in
31 DMF (2 mL) was added, and stirring was continued at room temperature overnight. Solvents
32 and volatiles were removed under reduced pressure, and the residue was dissolved in DCM (20
33 mL), washed with saturated $NaHCO_3$ (5 mL) and water (5 mL). After drying over anhydrous
34 Na_2SO_4 and concentration gave a residue was purified by silica gel chromatography (eluent: 3-
35 15% MeOH in DCM) to obtain compound **12** (1.6 g, 63 %). 1H NMR (400 MHz, DMSO- d_6) δ
36 11.29 (s, 1H), 7.89 – 7.84 (m, 2H), 7.81 (d, $J = 9.2$ Hz, 1H), 7.73 – 7.64 (m, 3H), 7.42 – 7.24
37 (m, 10H), 7.18 (s, 1H), 7.11 (d, $J = 18.3$ Hz, 1H), 5.19 (d, $J = 9.2$ Hz, 2H), 5.10 (s, 1H), 4.96
38 (d, $J = 14.6$ Hz, 1H), 4.69 (dd, $J = 44.0, 16.7$ Hz, 1H), 4.47 (d, $J = 8.5$ Hz, 2H), 4.39 – 4.17 (m,
39 4H), 4.15 – 3.97 (m, 4H), 3.87 (dd, $J = 19.7, 9.1$ Hz, 1H), 3.69 (dd, $J = 8.2, 6.9$ Hz, 2H), 3.45
40 – 3.35 (m, 2H), 2.99 (dd, $J = 13.4, 6.9$ Hz, 2H), 2.11 – 1.85 (m, 12H), 1.73 (dd, $J = 26.6, 6.5$
41 Hz, 6H), 1.51 – 1.21 (m, 10H). $^{13}C\{^1H\}$ NMR (101 MHz, DMSO- d_6) δ 171.8, 170.0, 169.9,
42 169.6, 169.3, 168.7, 167.8, 164.3, 156.1, 150.9, 143.8, 141.8, 140.7, 135.8, 135.5, 128.5,
43 128.2, 128.0, 127.8, 127.6, 127.0, 125.1, 120.0, 108.2, 101.0, 70.5, 69.8, 68.6, 66.7, 66.6,
44 65.9, 65.3, 61.4, 54.9, 49.8, 49.3, 48.3, 47.7, 46.8, 39.5, 38.4, 35.0, 31.2, 29.5, 28.6, 23.0, 22.7,
45 21.8, 20.5, 13.6, 11.90. HRMS (ESI-TOF) m/z calcd. For $C_{56}H_{68}N_6O_{17}$; 1097.1814 and found
46 1097.4727 $[M+H]^+$.
47
48
49
50
51
52
53
54
55
56
57
58
59
60

***N*-ethylamino(NHFmoc)-C γ (S)[(2-*N*-acetyl galactosamino-3,4,6-tri-*O*-acetyl-1-*O*-butylcarboxy)amidobutyl]-*N*-[acetamido-*N*1-thyminy] glycine (**2**)**

Compound **12** (0.6 g, 0.6 mmol) was dissolved in MeOH containing Pd-C (1.0 g, 10 wt% wet, Degussa type) at 0° C and the reaction was hydrogenated under normal pressure by maintaining temp 20-25 °C for 1 h. After completion of reaction (monitored by TLC), reaction contents was filtered through celite, washed with MeOH and the combined filtrate was concentrated to afford **2** as a white solid (0.3 g, 50 %); ¹H NMR (400 MHz, DMSO-d⁶) δ 11.26 (s, 1H), 8.71 (s, 2H), 7.85 (d, *J* = 7.6 Hz, 2H), 7.74 (t, *J* = 5.2 Hz, 1H), 7.58 (d, *J* = 7.2 Hz, 1H), 7.40 – 7.28 (m, 3H), 5.21 (d, 1H), 4.97 (d, *J* = 11.2 Hz, 1H), 4.49 (d, *J* = 8.4 Hz, 1H), 4.43 (d, *J* = 8.6 Hz, 2H), 4.02 (s, 3H), 3.97 – 3.82 (m, 25H), 3.72 (dd, *J* = 21.6, 11.6 Hz, 2H), 3.54 (d, *J* = 13.2 Hz, 1H), 3.38 (dd, *J* = 16.4, 10.1 Hz, 5H), 3.26 (s, 2H), 3.20 – 3.12 (m, 1H), 3.01 (d, *J* = 5.5 Hz, 2H), 2.10 (s, 3H), 2.01 (m, *J* = 15.7 Hz, 6H), 1.89 (s, 4H), 1.75 (d, *J* = 15.1 Hz, 6H), 1.46 (m, *J* = 7.4 Hz, 8H), 1.23 (m, 2H). ¹³C{¹H} NMR (101 MHz, DMSO-d₆) δ 171.9, 171.5, 170.0, 169.7, 169.4, 168.5, 168.0, 167.3, 164.5, 151.0, 148.6, 142.4, 142.2, 139.9, 127.0, 124.2, 120.0, 108.0, 101.0, 70.5, 69.8, 68.7, 66.7, 61.4, 57.5, 51.3, 50.8, 50.0, 49.4, 48.5, 47.89, 46.6, 41.9, 39.5, 38.2, 35.0, 31.5, 30.4, 28.8, 28.6, 23.1, 22.8, 22.5, 22.1, 21.9, 20.6, 19.2, 18.1, 13.5, 11.9. HRMS (ESI-TOF) *m/z* calcd. For C₄₉H₆₂N₆O₁₇; 1006. 4171 and found 1029.4069 [M+Na]⁺.

Solid phase synthesis of GalNAc₃ conjugated PNA

The PNA oligomers were assembled on rink amide resin using Fmoc synthesis protocol from C-terminus to N-terminus direction. The PNA oligomers were synthesized on solid phase, by using Fmoc strategy.^{26,27} The resin-bound amine PNA oligomers (25 mg, 0.22 mmol/g) in DMF were reacted with corresponding PNA monomer A/T/G/C (3 eq) in the presence of HBTU (6 mg, 17 μ mol, 3 eq), HOBt (2 mg, 17 μ mol, 3 eq), and DIPEA (3 μ L, 17 μ mol, 3 eq). The reaction was done for 5 min in microwave at 65 °C and 25 W and then 6h at room temperature (Discover SPS Manual Microwave Peptide Synthesizer, CEM Corporation, NC). Excess reagents were removed by filtration and the resin was washed with DMF, DCM and MeOH.

After all the PNA monomers were coupled, the resin-bound 15 mer PNA oligomer (25 mg, 0.22 mmol/g) in DMF (1:1) was coupled with corresponding (GalNAc)₃ derivative acid **1** (40 mg, 17 μ mol 3 eq) in the presence of Pybop (9 mg, 17 μ mol 3 eq), HOBt (2 mg, 17 μ mol, 3 eq) and DIPEA (3 μ L, 17 μ mol 3 eq). The reaction was done for 10 min in microwave at 75 °C and 40 W and then 24 h at room temperature. Excess reagents were removed by filtration

1
2
3 and the resin was washed with DMF, DCM and MeOH. For synthesis of trivalent-
4 $[C^{\gamma}(S)\text{-GalNAc-T}]_3$ PNA oligomer **3**, the resin bound 12-mer was coupled with the
5 the
6 monomer **2** in three consecutive cycles of addition-deprotection. The resin was treated with
7
8 90% TFA in DCM (200 μL) and triisopropylsilane (10 μL) in cold for 10 min followed by
9
10 stirring for 1.5 to 2 h at room temperature. The resin was filtered out, and the filtrate was
11
12 concentrated. The residue was dissolved in methanol and the product was precipitated with
13
14 cold dry ether. It was dissolved in MilliQ water and purified by RP-HPLC using semi-
15
16 preparative C18 (10 \times 250 mm) column using water-acetonitrile solvent system gradient from
17
18 0.1% TFA in $\text{CH}_3\text{CN}:\text{H}_2\text{O}$ (5:95) to 0.1% TFA in $\text{CH}_3\text{CN}:\text{H}_2\text{O}$ (95:5) in 20 min, flow rate of
19
20 2 mL/min, monitoring at 260 nm wavelength.

21
22 **Temperature dependent UV absorbance for T_m measurement.** UV-melting experiments
23
24 were carried out on Varian Cary 300 UV spectrophotometer equipped with Peltier heating
25
26 system. The samples for T_m measurements were prepared by mixing the calculated amounts of
27
28 respective oligonucleotides in the stoichiometric ratio (1:1, duplex) in sodium cacodylate
29
30 buffer (10 mM) and NaCl (10 mM) at pH 7.2 to achieve a final strand concentration of 3 μM
31
32 for each strand. The samples were annealed by heating at 90 $^\circ\text{C}$ for 10 min. followed by slow
33
34 cooling to room temperature for 8-10 h and then refrigerated for 12 to 24 h. The samples (500
35
36 μL) were transferred to quartz cell and equilibrated at the starting temperature for 5 min. The
37
38 OD at 260 nm was recorded from 20-92 $^\circ\text{C}$ with temperature ramping of 1 $^\circ\text{C}/\text{min}$. Each
39
40 melting experiment was repeated at least twice. From the plot of normalized absorbance at 260
41
42 nm as a function of the temperature, the T_m was determined from maximum in its first
43
44 derivative using Origin 8.5. The concentrations of all oligonucleotides were calculated from
45
46 absorbance and the molar extinction coefficients of the corresponding nucleobases i.e. T = 8.8
47
48 $\text{cm}^2/\mu\text{mol}$; C = 6.6 $\text{cm}^2/\mu\text{mol}$; G = 11.7 $\text{cm}^2/\mu\text{mol}$ and A = 13.7 $\text{cm}^2/\mu\text{mol}$.^{37,38}

46
47 **Circular dichroism.** CD spectra were recorded on JASCO J-815 spectropolarimeter. The
48
49 duplexes were constituted as described above. The CD spectra were recorded as an
50
51 accumulation of 3 scans from 300 to 190 nm using 1 mm cell, band-width of 1 nm, response
52
53 of 1 sec with resolution of 0.1 nm and a scan speed of 100 nm/min.

54
55 **Fluorescence spectroscopy.** UV-Visible spectra for all PNA oligomers and complementary
56
57 oligonucleotides were recorded on Perkin Elmer Lambda-45 UV-Visible Spectrophotometer
58
59 and fluorescence spectra were recorded on Horiba Jobin Yvon Fluorolog 3 spectrophotometer.
60
The samples for fluorescence spectra were prepared by mixing calculated amounts of PNA and
DNA in stoichiometric ratio (1:1 for duplex) in sodium cacodylate buffer (10 mM) and NaCl

1
2
3 (10 mM) at pH 7.2 to achieve a final strand concentration of 3 μ M for each strand. The annealed
4 samples were used to record fluorescence spectra at ambient temperature with λ_{ex} 458 and 484
5 nm and λ_{em} 520 nm with excitation slit width of 1 nm and emission slit width of 6 nm.
6
7

8
9 **Cell Permeation study.** HEK293 cells without any ASGPR as negative control were obtained
10 from American Type Culture Collection (ATCC, CRL-1573). HepG2 cells (ATCC HB-8065)
11 having ASGPR on cell surface were procured from National Centre for Cell Science (NCCS),
12 Cell Repository, Pune. The cells were cultured using Eagle's minimum essential medium
13 (MEM), which was supplemented with 10% fetal bovine serum (FBS, Sigma Aldrich). The
14 cells were incubated at 37°C with 5% CO₂ and maintained at the exponential growth phase.
15 About 1-2 million cells were transferred to the new flask and the cells were split. The medium
16 was discarded, and the cells were gently washed with 2 mL of sterile phosphate buffered saline
17 (PBS). Following PBS wash, the adhered cells were treated with 3 mL of 0.25% trypsin and
18 0.2% EDTA. After trypsin treatment for about 3 minutes at 37°C, 8 mL cell medium was added
19 to stop trypsinization. The concentration of live cells was estimated using a cell counter. The
20 cells suspension was centrifuged to and the pellet was resuspended in MEM. Finally, 1-2
21 million cells were passaged to a new flask.
22
23
24
25
26
27
28
29
30
31

32 **Confocal laser scanning microscopy analysis**

33
34
35 The cells were seeded in 35 x 15 mm cell imaging dishes containing 500 μ L MEM with
36 10% FBS and allowed to grow at 37°C in a humidified atmosphere containing 5% CO₂ for at
37 least 24 h. After the cells have grown to reach 50% confluency they were treated with PNAs.
38 The media from all the imaging dishes were discarded carefully and 500 μ L fresh media
39 containing respective 5(6)-carboxyfluorescein tagged PNAs (4 μ M) to the corresponding
40 dishes. The adhered cells were incubated at 37°C under 5% CO₂ for another 24 h. After
41 treatment with PNAs, the medium was carefully aspirated out and the adhered cells were
42 washed with PBS three times. The cells were then replenished with 500 μ L. Prior to imaging,
43 20 μ L of DAPI was added to stain the nuclei of the cells. The confocal microscopy imaging
44 has been repeated at least twice for each PNA.
45
46
47
48
49
50
51
52

53 Imaging of cells treated with caboxyfluorescein tagged PNAs were done on Leica TCS
54 SP8 microscope. The pin hole was set to 1 airy unit. For visualization of internalized PNAs,
55 the carboxyfluorescein dye tagged to the PNAs were excited with 514 nm laser and the
56 fluorescence emission signals from the molecules were detected from 550 nm to 660 nm using
57 the HyD detector. For visualization of nuclei, DAPI was excited at 405 nm with UV laser and
58
59
60

1
2
3 the signals over the range of 420 nm to 500 nm were detected. Bright field images were
4 captured using UV laser illumination and PMT detector.
5
6

7 **Flow cytometry**

8
9 HepG2 cells were seeded in a 12-well plate (1×10^5 cells/well) and cultured for 24
10 hours in DMEM, which was supplemented with 10% fetal bovine serum (FBS, Sigma Aldrich)
11 at 37°C with 5% CO₂. Then, media were removed and replaced with fresh media containing
12 either no PNA or 4 μM PNA. After an incubation period of 12 hours, the media from all the
13 wells were discarded and the cells were washed with cold PBS containing 2 mM EDTA and
14 harvested by trypsinization. The detached cells were diluted and suspended in PBS. The cells
15 were then analyzed using BD FACS celesta (BD Biosciences, San Jose, CA, USA).
16
17
18
19
20
21

22 **MTT assay**

23
24 HepG2 cells were seeded in a 96-well plate with a density of 1×10^4 cells/well, each
25 containing 100 μL of DMEM. After culturing them overnight at 37 °C in a 5% CO₂ incubator,
26 they were treated the PNAs (4 μM). Untreated cells were used as controls. After an incubation
27 of 12 hours, the media was discarded. Fresh media (96 μL) was added to all the wells. Then, 4
28 μL of MTT solution (1 mg/mL) was added to each well and the cells were incubated for 4 h at
29 37 °C in a 5% CO₂ incubator. Finally, the media was discarded and 100 μL of the DMSO was
30 added to each well to solubilize the formazan crystals. After 1 hour, absorbance at 570 nm was
31 measured using EnSight multimode plate reader (Perkin Elmer, USA).
32
33
34
35
36
37

38 **Acknowledgment.** P.B thanks UGC for the award of research fellowship. The authors thank
39 Dr Raghavendra Kikkeri, IISER Pune for permission to use lab facilities for biological studies.
40 P. J. thanks IISER Pune for research fellowship. B. M. and H.N. acknowledges IISER Tirupati
41 for post doctoral fellowship.
42
43
44
45

46 **ASSOCIATED CONTENT**

47 **Supporting Information:** The Supporting Information is available free of charge.

48 Schemes for synthesis of known compounds, ¹H and ¹³C NMR spectra of all new synthetic
49 compounds and key intermediates, HRMS of new compounds, HPLC and MALDI-TOF
50 spectral data of all PNA oligomers
51
52
53
54

55 **AUTHOR INFORMATION**

56 **Corresponding Author**
57
58
59
60

1
2
3 Krishna N Ganesh, Indian Institute of Science Education and Research, Karkambadi Road,
4 Mangalam, Tirupati 517507, India. orcid.org/0000-0003-2292-643X, Email:

5
6 kn.ganesh@iisertirupati.ac.in
7
8

9 **Authors contributions**

10 P. B., Chemical synthesis, Biophysical studies, Indian Institute of Science Education and
11 Research (IISER) Pune, Dr Homi Bhabha Road, Pune 411008
12
13

14
15 B. M. and H. N. B., Cell uptake experiments, Indian Institute of Science Education and
16 Research (IISER) Tirupati, Karkambadi Road, Tirupati 517507, Andhra Pradesh, India
17

18 B. M. and P. J., Fluorescence cytometry and MTT assay experiments
19

20
21 M. M. Alnylam Pharmaceuticals, Boston, USA and K. N. G. IISER, Pune and IISER,
22 Tirupati, Design of experiments and Project Investigators
23
24

25 **References**

26
27
28 1. van der Ree, M. H.; de Vree, J. M.; Stelma, F.; Willemse, S.; van der Valk, M.; Rietdijk,
29 S.; Molenkamp, R.; Schinkel, J.; van Nuenen, A. C.; Beuers, U.; Hadi, S.; Harbers, M.; van der
30 Veer, E.; Liu, K.; Grundy, J.; Patick, A. K.; Pavlicek, A.; Blem, J.; Huang, M.; Grint, P.; Neben,
31 S.; Gibson, N. W.; Kootstra, N. A.; Reesink, H. W. Safety, tolerability, and antiviral effect of
32 RG-101 in patients with chronic hepatitis C: a phase 1B, double-blind, randomised controlled
33 trial. *Lancet* **2017**, *389*, 709–717.
34
35

36
37
38 2. Rottiers, V.; Obad, S.; Petri, A.; McGarrah, R.; Lindholm, M. W.; Black, J. C.; Sinha,
39 S.; Goody, R. J.; Lawrence, M. S.; deLemos, A. S.; Hansen, H. F.; Whittaker, S.; Henry, S.;
40 Brookes, R.; Najafi-Shoushtari, S. H.; Chung, R. T.; Whetstine, J. R.; Gerszten, R. E.;
41 Kauppinen, S.; Näär, A. M. Pharmacological inhibition of a microRNA family in nonhuman
42 primates by a seed-targeting 8-mer antimir. *Sci. Transl. Med.* **2013**, *5*, 212ra162.
43
44

45
46 3. Janssen, H. L.; Reesink, H. W.; Lawitz, E. J.; Zeuzem, S.; Rodriguez-Torres, M.;
47 Patel, K.; van der Meer, A. J.; Patick, A. K.; Chen, A.; Zhou, Y.; Persson, R.; King, B. D.;
48 Kauppinen, S.; Levin, A. A.; Hodges, M. R. Treatment of HCV infection by targeting
49 microRNA. *N. Engl. J. Med.* **2013**, *368*, 1685–1695.
50
51

52
53 4. Wittrup, A.; Lieberman, J. Knocking down disease: a progress report on siRNA
54 therapeutics. *Nat. Rev. Genet.* **2015**, *16*, 543–552.
55
56

57
58 5. Whitehead, K. A.; Langer, R.; Anderson, D. G. Knocking down barriers: advances in
59 siRNA delivery. *Nat. Rev. Drug Discov.* **2009**, *8*, 129–138.
60

1
2
3
4
5
6
7
8
9
10
11
12
13
14
15
16
17
18
19
20
21
22
23
24
25
26
27
28
29
30
31
32
33
34
35
36
37
38
39
40
41
42
43
44
45
46
47
48
49
50
51
52
53
54
55
56
57
58
59
60

6. Nair, J. K.; Willoughby, J. L.; Chan, A.; Charisse, K.; Alam, M. R.; Wang, Q.; Hoekstra, M.; Kandasamy, P.; Kel'in, A. V.; Milstein, S.; Taneja, N.; O'Shea, J.; Shaikh, S.; Zhang, L.; van der Sluis, R. J.; Jung, M. E.; Akinc, A.; Hutabarat, R.; Kuchimanchi, S.; Fitzgerald, K.; Zimmermann, T.; van Berkel, T. J. C.; Maier, M. A.; Rajeev, K. G.; Manoharan, M. Multivalent N-acetylgalactosamine-conjugated siRNA63 localizes in hepatocytes and elicits robust RNAi-mediated gene silencing. *J. Am. Chem. Soc.* **2014**, *136*, 16958–16961.

7. Prakash, T. P.; Graham, M. J.; Yu, J.; Carty, R.; Low, A.; Chappell, A.; Schmidt, K.; Zhao, C.; Aghajan, M.; Murray, H. F.; Riney, S.; Booten, S. L.; Murray, S. F.; Gaus, H.; Crosby, J.; Lima, W. F.; Guo, S.; Monia, B. P.; Swayze, E. E.; Seth, P. P. Targeted delivery of antisense oligonucleotides to hepatocytes using triantennary N-acetyl galactosamine improves potency 10-fold in mice. *Nucleic Acids Res.* **2014**, *42*, 8796–8807.

8. Tanowitz, M.; Hettrick, L.; Revenko, A.; Kinberger, G. A.; Prakash, T. P.; Seth, P. P. Asialoglycoprotein receptor 1 mediates productive uptake of N-acetylgalactosamine-conjugated and unconjugated phosphorothioate antisense oligonucleotides into liver hepatocytes. *Nucleic Acids Res.* **2017**, *45*, 12388–12400.

9. Steirer, L. M.; Park, E. I.; Townsend, R. R.; Baenziger, J. U. The asialoglycoprotein receptor regulates levels of plasma glycoproteins terminating with sialic acid α 2,6-galactose. *J. Biol. Chem.* **2009**, *284*, 3777–3783.

10. Huang, X.; Leroux, J. C.; Castagner, B. Well-defined multivalent ligands for hepatocytes targeting via asialoglycoprotein receptor. *Bioconjug. Chem.* **2017**, *28*, 283–295.

11. Scott, L. J. Givosiran: First Approval. *Drugs* **2020**, *80*, 335–339.

12. Egholm, M.; Buchardt, O.; Christensen, L.; Behrens, C.; Freier, S.M.; Driver, D. A.; Berg, R. H.; Kim, S. K.; Norden, B.; Nielsen, P. E. PNA hybridizes to complementary oligonucleotides obeying the Watson-Crick hydrogen-bonding rules. *Nature* **1993**, *365*, 566–568

13. Jensen, K. K.; Qrum, H.; Nielsen, P. E.; Norden, B. Kinetics for hybridization of peptide nucleic acids (PNA) with DNA and RNA studied with the BIAcore technique. *Biochemistry* **1997**, *36*, 5072–5077.

14. Ganesh, K. N.; Nielsen, P. E. Peptide nucleic acids: analogs and derivatives. *Curr. Org. Chem.* **2000**, *4*, 931–943.

- 1
2
3 15. Kumar, V. A.; Ganesh, K. N. Conformationally constrained PNA analogues:
4 Structural evolution toward DNA/RNA binding selectivity. *Acc. Chem. Res.* **2005**, *38*, 404–
5 412.
6
7
8
9 16. Kumar, V. A.; Ganesh, K. N. Structure-editing of nucleic acids for selective
10 targeting of RNA. *Curr. Top Med. Chem.* **2007**, *7*, 715–726.
11
12
13 17. Jain, D. R.; Anandi V, L.; Lahiri, M.; Ganesh, K. N. Influence of pendant chiral C γ -
14 (alkylideneamino/guanidino) cationic side-chains of PNA backbone on hybridization with
15 complementary DNA/RNA and cell permeability. *J. Org. Chem.* **2014**, *79*, 9567–9577.
16
17
18 18. Sahu, B.; Chenna, V.; Lathrop, K. L.; Thomas, S. M.; Zon, G.; Livak, K. J.; Ly, D.
19 H. Synthesis of conformationally preorganized and cell-permeable guanidine-based γ -peptide
20 nucleic acids (γ GPNA). *J. Org. Chem.* **2009**, *74*, 1509–1516.
21
22
23 19. Moccia, M.; Adamo, M. F. A.; Saviano, M. Insights on chiral, backbone modified
24 peptide nucleic acids: Properties and biological activity. *Artif. DNA PNA XNA* **2014**, *5*,
25 e110716.
26
27
28
29 20. Biessen, E. A.; Sliedregt-Bol, K.; T' Hoen, P. A.; Prince, P.; Van der Bilt, E.;
30 Valentijn, A. R.; Meeuwenoord, N. J.; Princen, H.; Bijsterbosch, M. K.; Van der Marel, G.
31 A.; Van Boom, J. H.; Berkel, T. J. Design of a targeted peptide nucleic acid prodrug to inhibit
32 hepatic human microsomal triglyceride transfer protein expression in hepatocytes. *Bioconjug.*
33 *Chem.* **2002**, *13*, 295–302.
34
35
36
37 21. Van Rossenberg, S. M.; Sliedregt-Bol, K. M.; Prince, P.; Van Berkel, T. J.; Van
38 Boom, J. H.; Van der Marel, G. A.; Biessen, E. A. A targeted peptide nucleic acid to down-
39 regulate mouse microsomal triglyceride transfer protein expression in hepatocytes.
40 *Bioconjug. Chem.* **2003**, *14*, 1077–1082.
41
42
43
44 22. Ostergaard, M. E.; Yu, J.; Kinberger, G. A.; Wan, W. B.; Migawa, M. T.; Vasquez,
45 G.; Schmidt, K.; Gaus, H. J.; Murray, H. M.; Low, A.; Swayze, E. E.; Prakash, T. P.; Seth, P.
46 P. Efficient synthesis and biological evaluation of 5'-GalNAc conjugated antisense
47 oligonucleotides. *Bioconjug. Chem.* **2015**, *26*, 1451–1455.
48
49
50
51 23. Nielsen, P. E.; Egholm, M.; Berg, R. H.; Buchardt, O. Sequence-selective recognition
52 of DNA by strand displacement with a thymine-substituted polyamide. *Science* **1991**, *254*,
53 1497–1500.
54
55
56
57
58
59
60

- 1
2
3
4
5
6
7
8
9
10
11
12
13
14
15
16
17
18
19
20
21
22
23
24
25
26
27
28
29
30
31
32
33
34
35
36
37
38
39
40
41
42
43
44
45
46
47
48
49
50
51
52
53
54
55
56
57
58
59
60
24. Wojciechowski, F.; Hudson, R. H. E. A convenient route to *N*-[2-(Fmoc)aminoethyl]glycine esters and PNA oligomerization using a bis-*N*-Boc nucleobase protecting group strategy. *J. Org. Chem.* **2008**, *73*, 3807–3816.
25. Porcheddu, A.; Giacomelli, G.; Piredda, I.; Carta, M.; Nieddu, G. A practical and efficient approach to PNA monomers compatible with Fmoc mediated solid phase synthesis protocols. *Eur. J. Org. Chem.* **2008**, *34*, 5786–5797.
26. Christensen, L.; Fitzpatrick, R.; Gildea, B.; Petersen, K. H.; Hansen, H. F.; Koch, T.; Egholm, M.; Buchardt, O.; Nielsen, P. E.; Coull, J.; Berg, R. H. Solid-phase synthesis of peptide nucleic acids. *J. Peptide Sci.* **1995**, *3*, 175–183.
27. Erickson, B. W.; Merrifield, R. B. *Solid Phase Peptide Synthesis. In the Proteins*, Vol. II, 3rd ed. Neurath, H.; Hill, R. L. eds. Academic Press, New York, **1976**, 255.
28. Prakash, T. P.; Yu, J.; Migawa, M. T.; Kinberger, G. A.; Wan, W. B.; Østergaard, M. E.; Carty, R. L.; Vasquez, G.; Low, A.; Chappell, A.; Schmidt, K.; Aghajan, M.; Crosby, J.; Murray, H. M.; Booten, S. L.; Hsiao, J.; Soriano, A.; Machemer, T.; Cauntay, P.; Burel, S. A.; Murray, S. F.; Gaus, H.; Graham, M. J.; Swayze, E. E.; Seth, P. P. Comprehensive structure–activity relationship of triantennary *N*-acetylgalactosamine conjugated antisense oligonucleotides for targeted delivery to hepatocytes. *J. Med. Chem.* **2016**, *59*, 2718–2733.
29. Sharma, V. K.; Osborn, M. F.; Hassler, M. R.; Echeverria, D.; Ly, S.; Ulashchik, E. A.; Martynenko-Makaev, Y. V.; Shmanai, V. V.; Zatsepin, T. S.; Khvorova, A. and Watts, J. K. A. Novel cluster and monomer-based GalNAc structures induce effective uptake of siRNAs in vitro and in vivo. *Bioconjug. Chem.* **2018**, *29*, 2478–2488.
30. Van Den Hamer, C. J. A.; Morell, A. G.; Scheinberg, I. H.; Hickman, J.; Ashwell, G. Physical and chemical studies on ceruloplasmin IX. The role of galactosyl residues in the clearance of ceruloplasmin from the circulation. *J. Biol. Chem.* 1970, *245*, 4397–4402.
31. Ashwell, G.; Harford, J. Carbohydrate-specific receptors of the liver. *Annu. Rev. Biochem.* 1982, *51*, 531–554.
32. Meier, M.; Bider, M. D.; Malashkevich, V. N.; Spiess, M.; Burkhard, P. Crystal structure of the carbohydrate recognition domain of the H1 subunit of the asialoglycoprotein receptor. *J. Mol. Biol.* **2000**, *300*, 857–865.
33. Sanhueza, C. A.; Baksh, M. M.; Thuma, B.; Roy, M. D.; Dutta, S.; Prévile, C.; Chrnyk, B. A.; Beaumont, K.; Dullea, R.; Ammirati, M.; Liu, S.; Gebhard, D.; Finley, J. E.; Salatto, C. T.; King-Ahmad, A.; Stock, I.; Atkinson, K.; Reidich, B.; Lin, W.; Kumar, R.; Tu,

1
2
3 M.; Menhaji-Klotz, E.; Price, D. A.; Liras, S.; Finn, M. G.; Mascitti, V. Efficient liver
4 targeting by polyvalent display of a compact ligand for the asialoglycoprotein receptor. *J Am*
5 *Chem Soc.* **2017**, *139*, 3528–3536.
6
7

8
9 34. Shigeo, M.; Kristofer, K.; Jayaprakash, K. N.; Klaus C.; Rajar, M. M.; Kretschmer,
10 P.; Chang, G. P.; Kel'in, A. V.; Kandasamy, P.; Willoughby, J. L. S.; Liebow, A.; Querbes,
11 W.; Yucius, K.; Nguyen, T.; Milstein, S.; Maier, M. A.; Rajeev, K. G.; Manoharan, M.
12 siRNA conjugates carrying sequentially assembled trivalent N-acetylgalactosamine linked
13 through nucleosides elicit robust gene silencing in vivo in hepatocytes. *ACS Chem. Biol.*
14 **2015**, *10*, 1181–1187.
15
16
17
18

19
20 35. Rajeev, K. G.; Nair, J.K.; Jayaraman, M.; Charisse, K.; Taneja, N.; O'Shea, J.;
21 Willoughby, J. L. S.; Yucius, K.; Nguyen, T.; Shulga-Morskaya, S.; Milstein, S.; Liebow, A.;
22 Querbes, W.; Borodovsky, A.; Fitzgerald, K.; Maier, M. A.; Manoharan, M. Hepatocyte-
23 specific delivery of siRNAs conjugated to novel non-nucleosidic trivalent N-
24 acetylgalactosamine elicits robust gene silencing in vivo. *ChemBioChem* **2015**, *16*, 903–908.
25
26
27
28

29
30 36. Schmidt, K.; Prakash, T. P.; Donner, A. J.; Kinberger, G. A.; Gaus, H. J.; Low, A.;
31 Østergaard, M. E.; Bell, M.; Swayze, E. E.; Seth, P. P. Characterizing the effect of GalNAc
32 and phosphorothioate backbone on binding of antisense oligonucleotides to the
33 asialoglycoprotein receptor *Nucleic Acids Res.* **2017**, *45*, 2294-2306.
34
35
36

37
38 37. Cavaluzzi, M. J.; Borer, P. N. Revised UV extinction coefficient for nucleoside-5'-
39 monophosphates and unpaired DNA and RNA. *Nucleic Acids Res.* **2004**, *32*, e13.
40
41

42 38. Kallansrud, G.; Ward, B. A comparison of measured and calculated single- and
43 double-stranded oligodeoxynucleotide extinction coefficients. *Anal. Biochem.* **1996**, *236*,
44 134–138.
45
46
47
48
49
50
51
52
53
54
55
56
57
58
59
60